Walking in the Hidden Valley

Exploring near-conformal dark sector theories

Joshua Lockyer
joshua.lockyer@uni-graz.at

Collaboration with: Suchita Kulkarni & Matthew Strassler

Based on
arXiv:2502.18566

UNI GRAZ NAWI Graz Natural Sciences FWF

Confining Hidden Valley models

- Hidden Valley (HV) models extend the SM with a new dark sector uncharged under the SM gauge group, instead connecting to the SM through a heavy mediator, here we use a $U(1)$ Z′.

arXiv:0604261, M.J. Strassler et al.

arXiv:1502.05409, P. Schwaller et al.

arXiv:1503.00009, T. Cohen et al.
arXiv:0712.2041, T. Han et al.

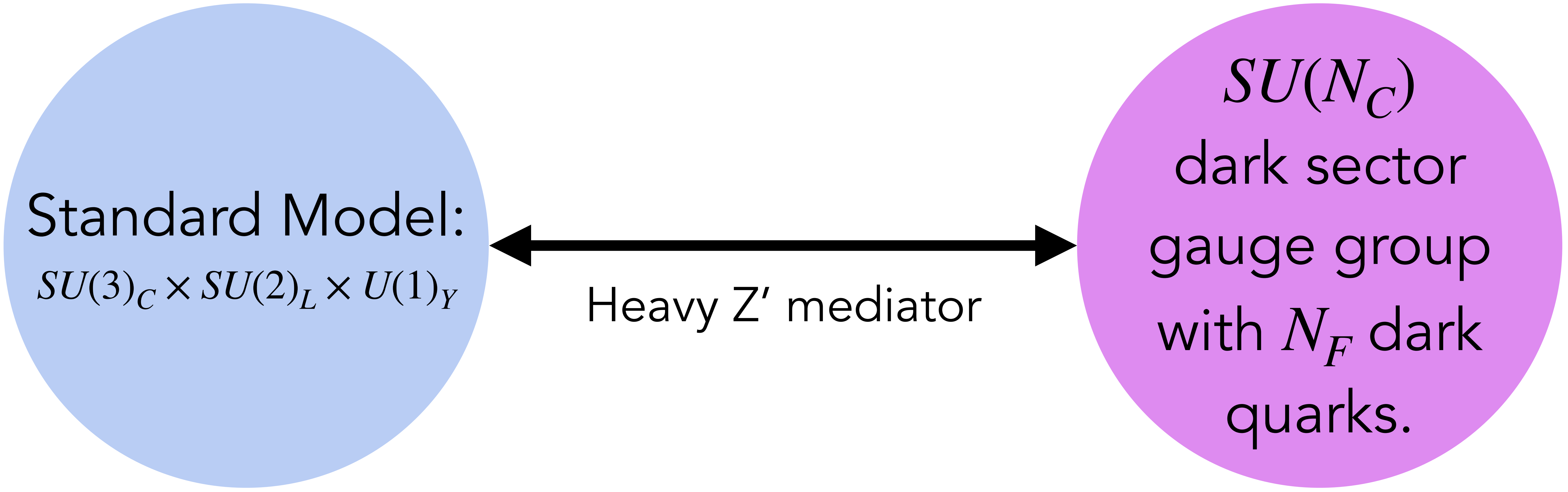

- Focus on dark sectors with a $SU(N_C)$ gauge group with N_F flavours of degenerate fundamental Dirac fermions (dark quarks). Such sectors are characterised by four parameters; N_C , N_F , Λ and m_{π_D}/Λ. Confinement ensures the formation of bound states; in our case dark mesons - typically dark pions or dark rhos.

- Certain classes of HV models at low N_F/N_C (resembling QCD) present novel collider signatures and exciting opportunities for new physics discovery. Theories with large N_F/N_C are an undeveloped area that could give rise to distinct signatures.

Anomalous jet signatures

arXiv:1503.00009 - T. Cohen et al.

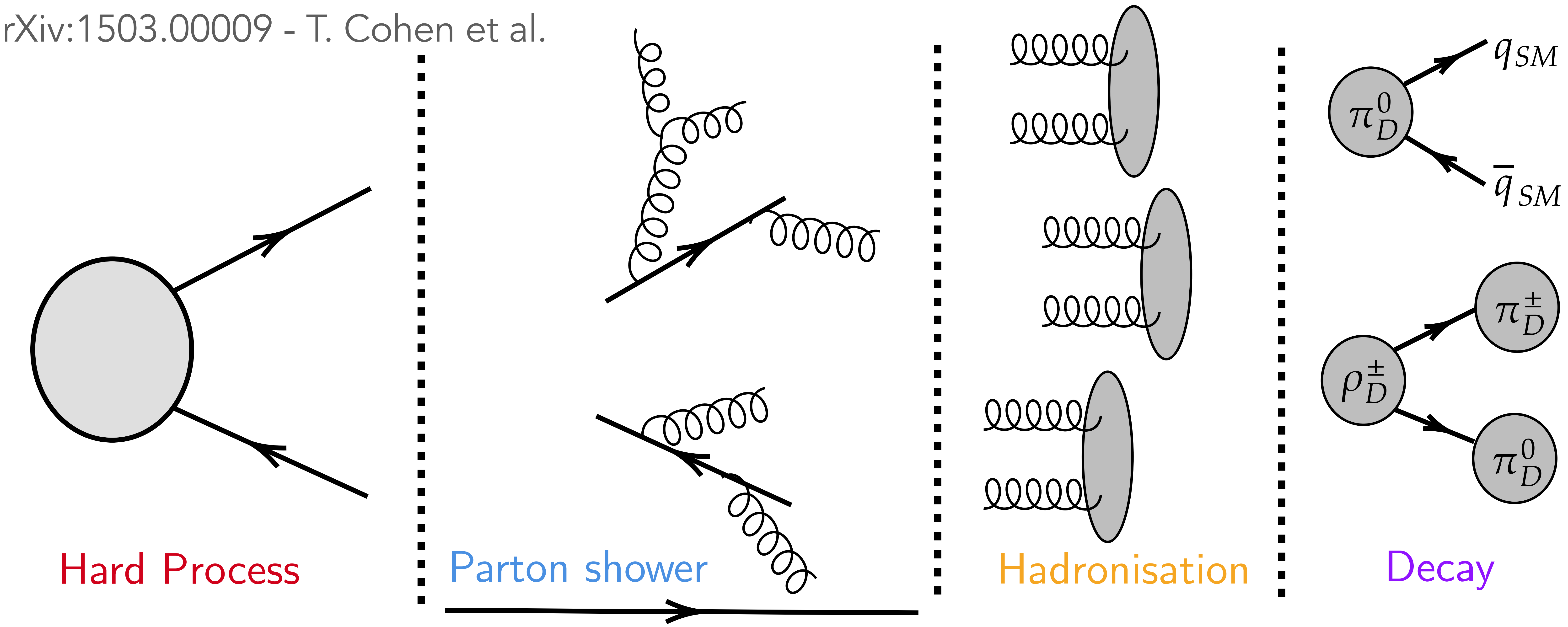

α runs, controlled by $N_F\,/\,N_C$ and Λ

- Production of initial dark partons can be initiated through a hard process at a collider, via the mediator.
- The initial dark partons undergo parton showering eventually reaching close to a characteristic energy scale where the shower stops and hadronisation occurs.

- A portion of dark mesons will decay to SM particles through the mediator, resulting in a jet with a mixture of stable dark hadrons and SM decay products.
- Typically these exotic jet signatures are known as "dark showers" and generically give rise to high multiplicity signatures which can have displaced vertices e.g. emerging or semi-visible jets that are well-known at small ratio of N_F/N_C.

Near-conformal dark sector models

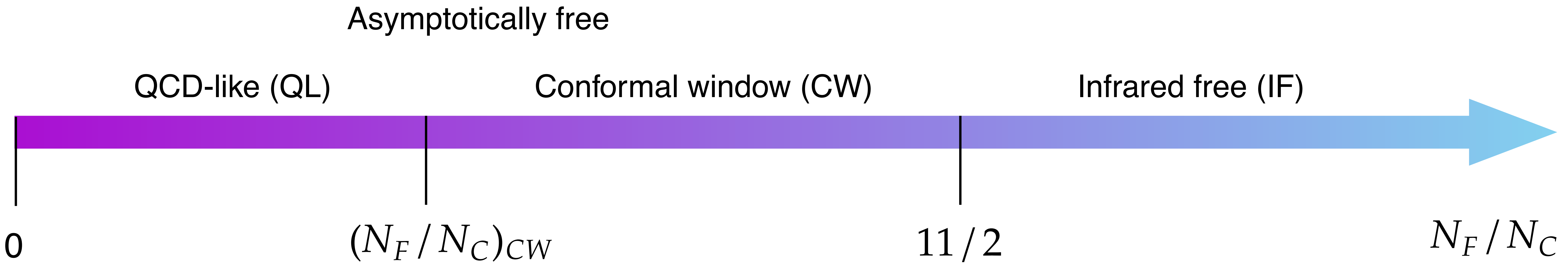

- For $N_F/N_C \geq \left(N_F/N_C\right)_{CW}$, the dark sector enters a "conformal window" (CW) - for a massless theory that is weakly coupled in the UV, the theory flows to an IR fixed point (IRFP). The theory is only strictly conformal for $\alpha(\mu_0) = \alpha_*$. Near the onset of the CW, the β function is hypothesised to become small over a large range of α - a "walking theory"

- Lots of work already done on the non-perturbative structure and the low-energy EFT descriptions of large N_F/N_C theories. Exact value of $\left(N_F/N_C\right)_{CW}$ still a matter of debate. Hadron spectrum very different from normal QCD - hadronisation not well understood/modelled within this region.

arXiv:2306.07236, A. Hasenfratz et al. arXiv:0902.3494, T. Appelquist et al. arXiv:2312.13761, R. Zwicky
arXiv:2008.12223, J.W. Lee arXiv:2312.08332, A. Pomarol et al. arXiv:0902.3494, F. Sannino

- Interesting phenomenology could occur for $M_q \neq 0, M_q \ll \Lambda$. If the amount of massive quarks is enough to push the IR theory out of the CW then exotic QL hadronisation occurs around $\mu \sim M_q$; QL hadronisation is also challenging but more familiar.

Near-conformal parton showering

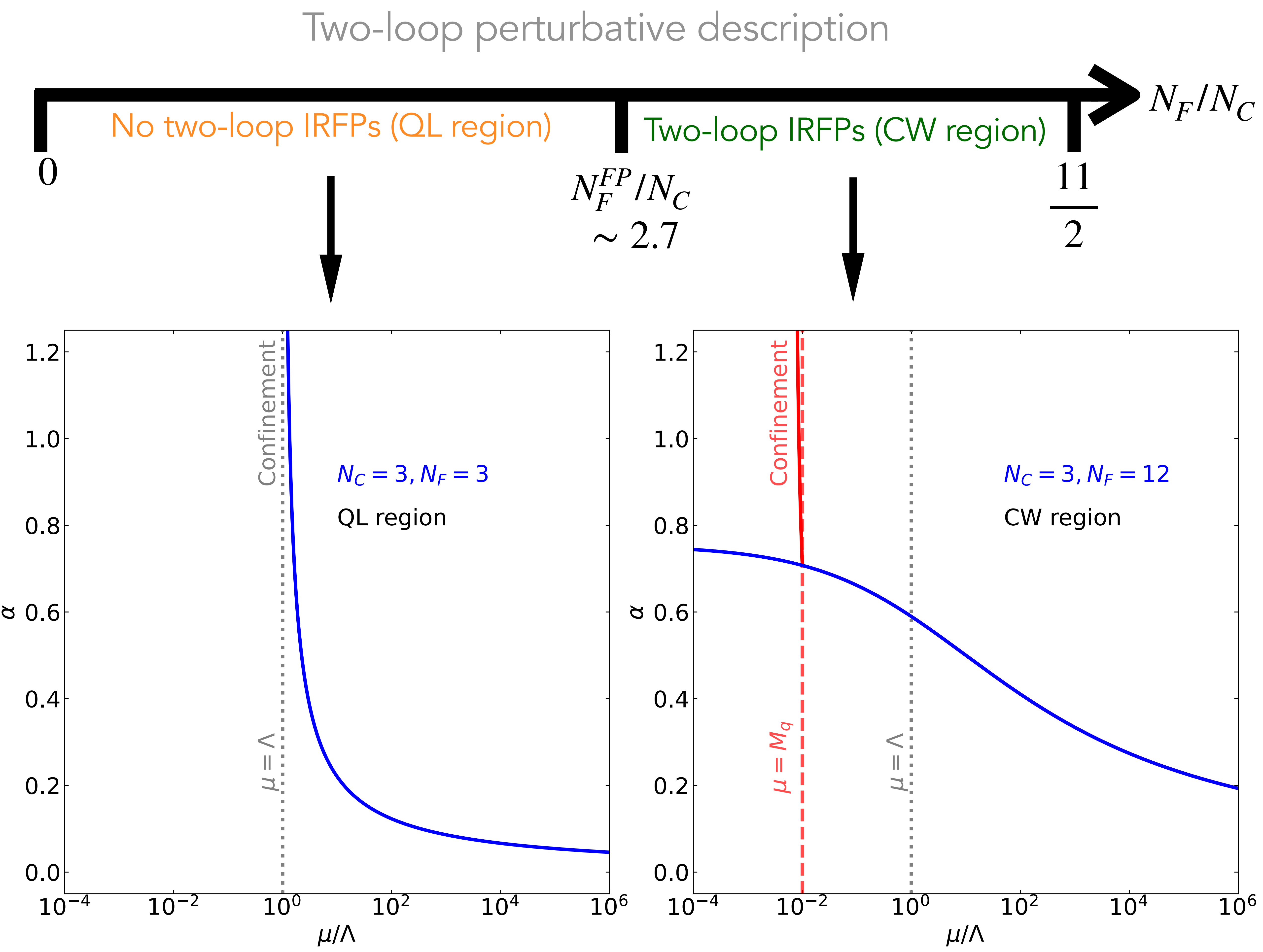

"Confinement" for illustrative purposes only

- For now, focus on parton showering at large N_F/N_C.
- The 't Hooft gauge coupling, $\lambda = \alpha N_C$, in part controls parton showering behaviour, where α is governed by the Renormalisation Group Equations (RGE),

$$\mu^2 \frac{d\alpha}{d\mu^2} = \beta(\alpha) = -\alpha^2 \left(\beta_0 + \beta_1 \alpha\right) \qquad \text{(at 2-loop)}$$

- At two-loop, for $N_F/N_C \gtrsim 2.7$, α flows to a non-trivial infra-red fixed point (IRFP); as N_F/N_C increases α begins to slow down.

Non-trivial fixed point: $\alpha_* = -\dfrac{\beta_0}{\beta_1}$; > 0 for $N_F/N_C \gtrsim 2.7$

- Choose to do parton showering with two-loop α - the first order IRFPs appear. New procedures are needed to understand parton showering within this region. T. Banks., A. Zaks, Nucl.Phys.B 196 ('82)

Improving upon the current procedure

- QL parton showering is parameterised by a scale Λ, indicating the divergence of the running coupling, below which the perturbative expansion breaks down. For SM QCD, Λ_{QCD} is a useful proxy for the scale of the theory. As such, to a good approximation, $\lambda = \alpha N_C$ is governed solely by N_F/N_C and μ/Λ.

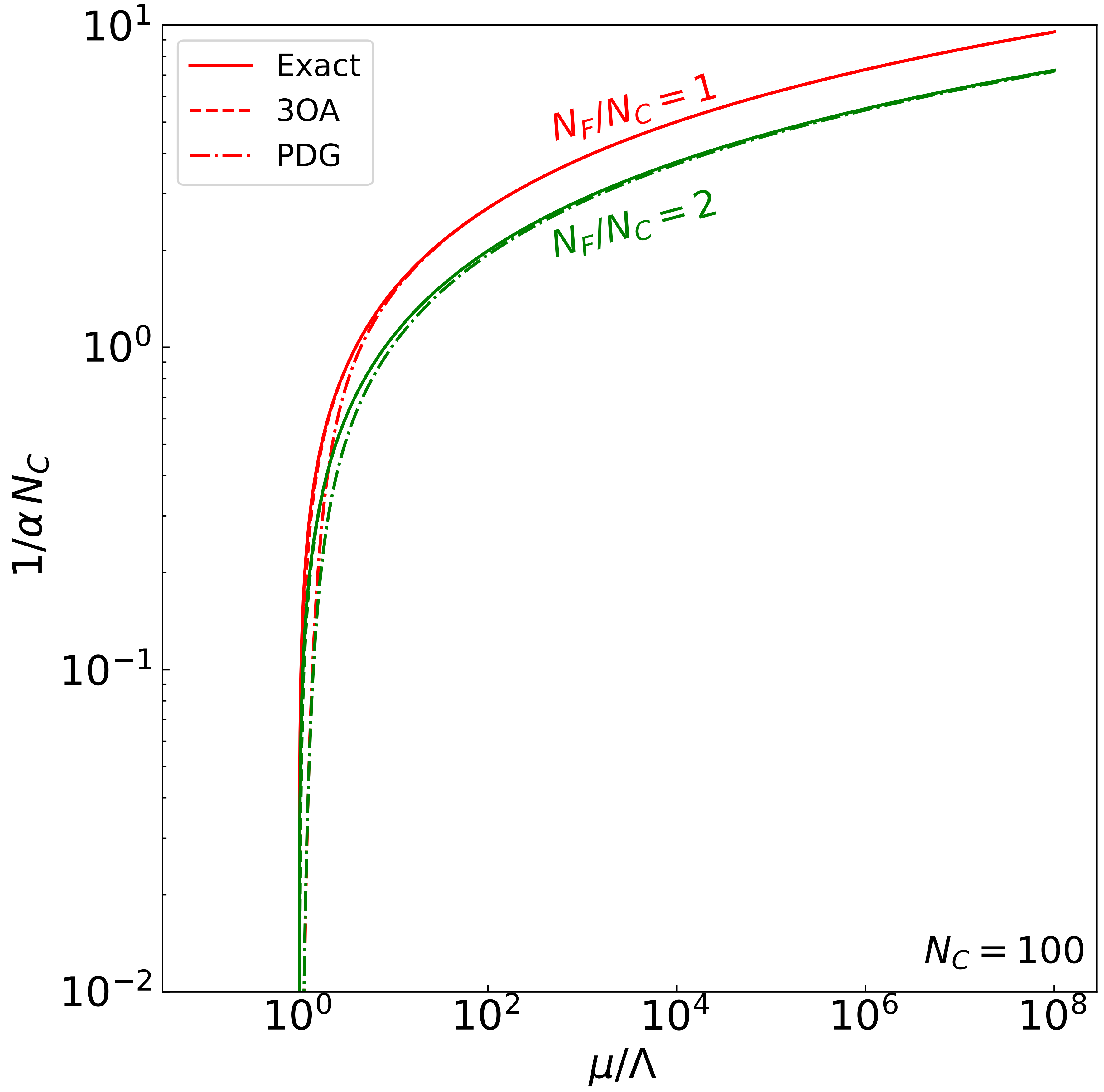

$$N_C\,\alpha = f(N_F/N_C, \mu/\Lambda) \; + \mathcal{O}(N_F/N_C^2) \text{ corrections}$$

- Due to the presence of the IRFP, this definition of Λ no longer works beyond $N_F/N_C \gtrsim 2.7$ and thus existing α approximations within event generators (the PDG formula) are insufficient to describe CW behaviour.

$$\alpha(\mu) = \frac{1}{\beta_0 \ln(\mu^2/\Lambda^2)} \left[1 + \frac{1}{\alpha_*} \frac{\ln[\ln(\mu^2/\Lambda^2)]}{\beta_0 \ln(\mu^2/\Lambda^2)} \right]$$

- In the CW region, at low μ/Λ, α takes on a power-law form. Hence Λ is not a proxy for the confinement scale, but rather characterises the crossover between power-law and logarithmic running behaviours in the CW region.

$$\alpha - \alpha_* \sim \left(\frac{\mu^2}{\Lambda^2}\right)^{\gamma} \quad ; \quad \gamma = \left.\frac{\partial \beta}{\partial \alpha}\right|_{\alpha=\alpha_*} = \beta_0 \alpha_* \qquad \text{(at 2-loop)}$$

Improving upon the current procedure

- QL parton showering is parameterised by a scale Λ, indicating the divergence of the running coupling, below which the perturbative expansion breaks down. For SM QCD, Λ_{QCD} is a useful proxy for the scale of the theory. As such, to a good approximation, $\lambda = \alpha N_C$ is governed solely by N_F/N_C and μ/Λ.

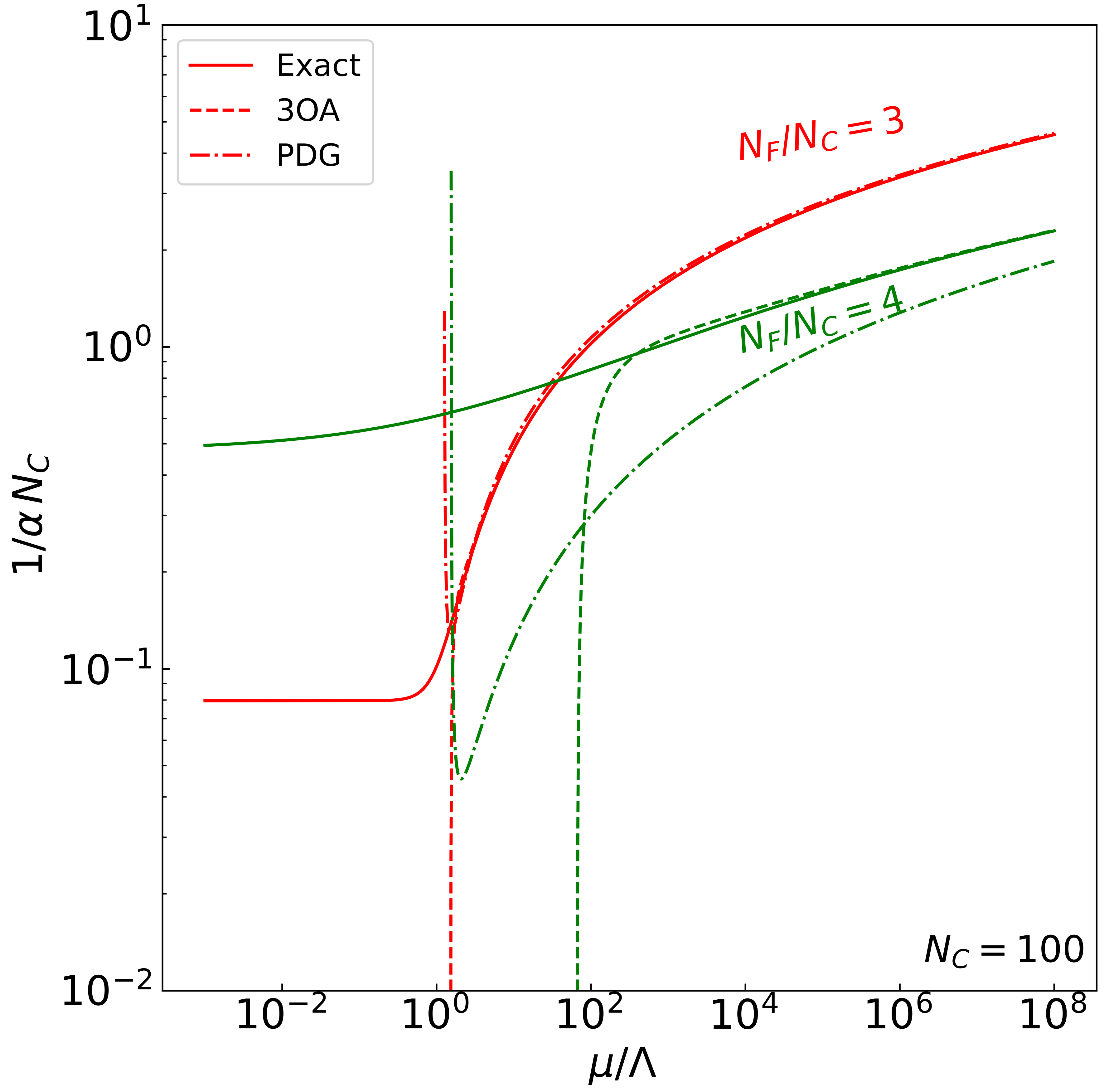

$$N_C\,\alpha = f(N_F/N_C, \mu/\Lambda) \; + \mathcal{O}(N_F/N_C^2) \text{ corrections}$$

- Due to the presence of the IRFP, this definition of Λ no longer works beyond $N_F/N_C \gtrsim 2.7$ and thus existing α approximations within event generators (the PDG formula) are insufficient to describe CW behaviour.

$$\alpha(\mu) = \frac{1}{\beta_0 \ln(\mu^2/\Lambda^2)}\left[1 + \frac{1}{\alpha_*}\frac{\ln[\ln(\mu^2/\Lambda^2)]}{\beta_0 \ln(\mu^2/\Lambda^2)}\right]$$

- In the CW region, at low μ/Λ, α takes on a power-law form. Hence Λ is not a proxy for the confinement scale, but rather characterises the crossover between power-law and logarithmic running behaviours in the CW region.

$$\alpha - \alpha_* \sim \left(\frac{\mu^2}{\Lambda^2}\right)^{\gamma} \quad ; \quad \gamma = \left.\frac{\partial \beta}{\partial \alpha}\right|_{\alpha=\alpha_*} = \beta_0\alpha_* \qquad \text{(at 2-loop)}$$

Monte Carlo implementation

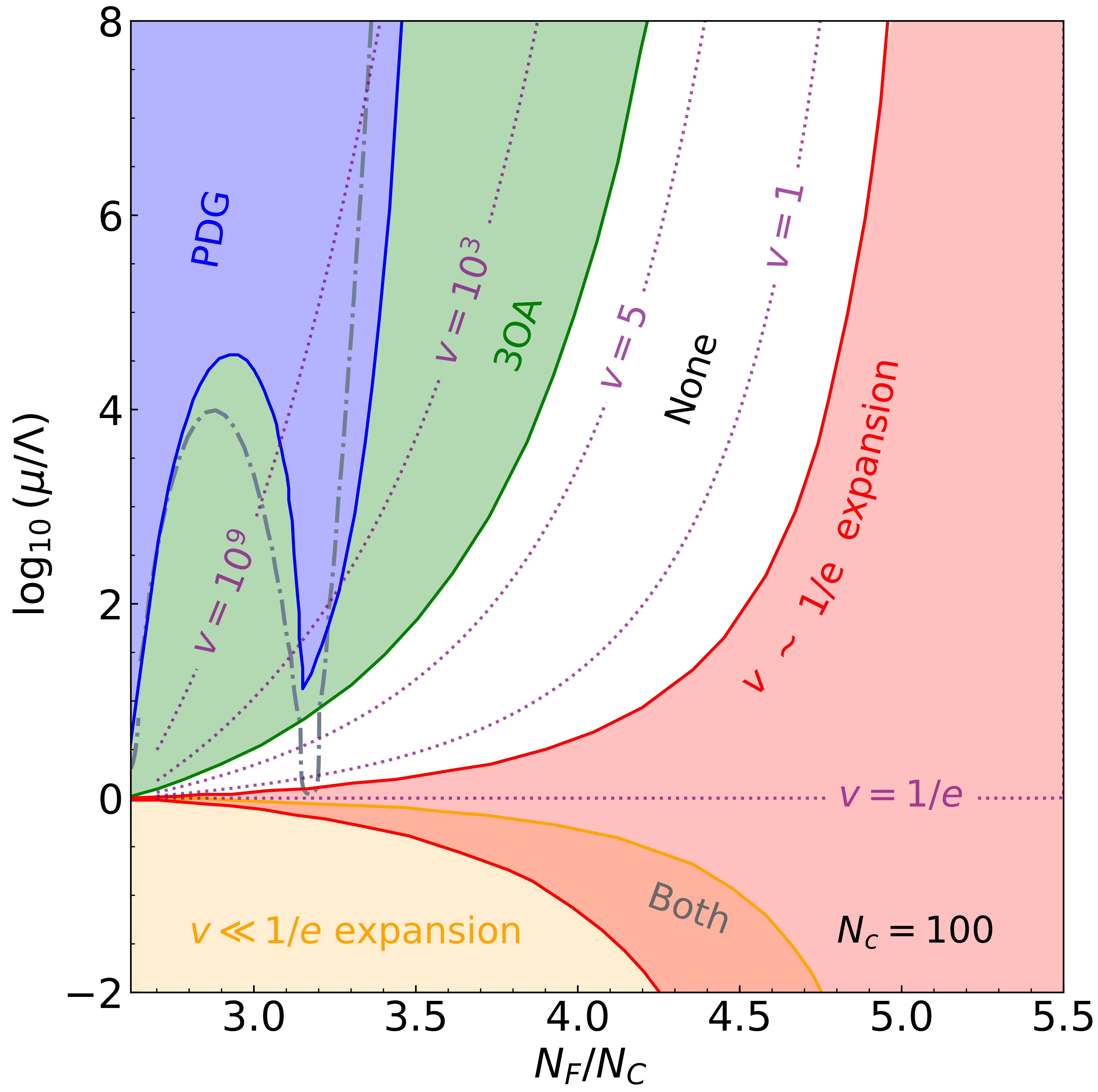

- By taking this IRFP into account, we have two RGE solutions that accurately describe α in both regions. From this, we can find the explicit forms in both regions in terms of the two real branches of the Lambert W function,

$$\alpha = \alpha_* \left[W_{-1}(-z) + 1\right]^{-1} \quad ; \quad \alpha = \alpha_* \left[W_0(z) + 1\right]^{-1} \quad ; \quad z = \frac{1}{e}\left(\frac{\mu^2}{\Lambda^2}\right)^{\beta_0 \alpha_*}$$

QL-region CW-region

- For large μ/Λ, use third order expansion (3OA) in both branches. For small μ/Λ, use Taylor expansions around $z = 0$ and $z = 1/e$. Examining the validity (deviation $\geq 2\%$) of these expansions reveals a large area of parameter space covered by none.

- These expansions fail when the running coupling is slow - natural to interpolate. The best solution, in the CW region, was to use a 3OA where applicable and linearly interpolate in the regions where it fails. The 3OA approximation suffices in the QL region.

Sudakov algorithm

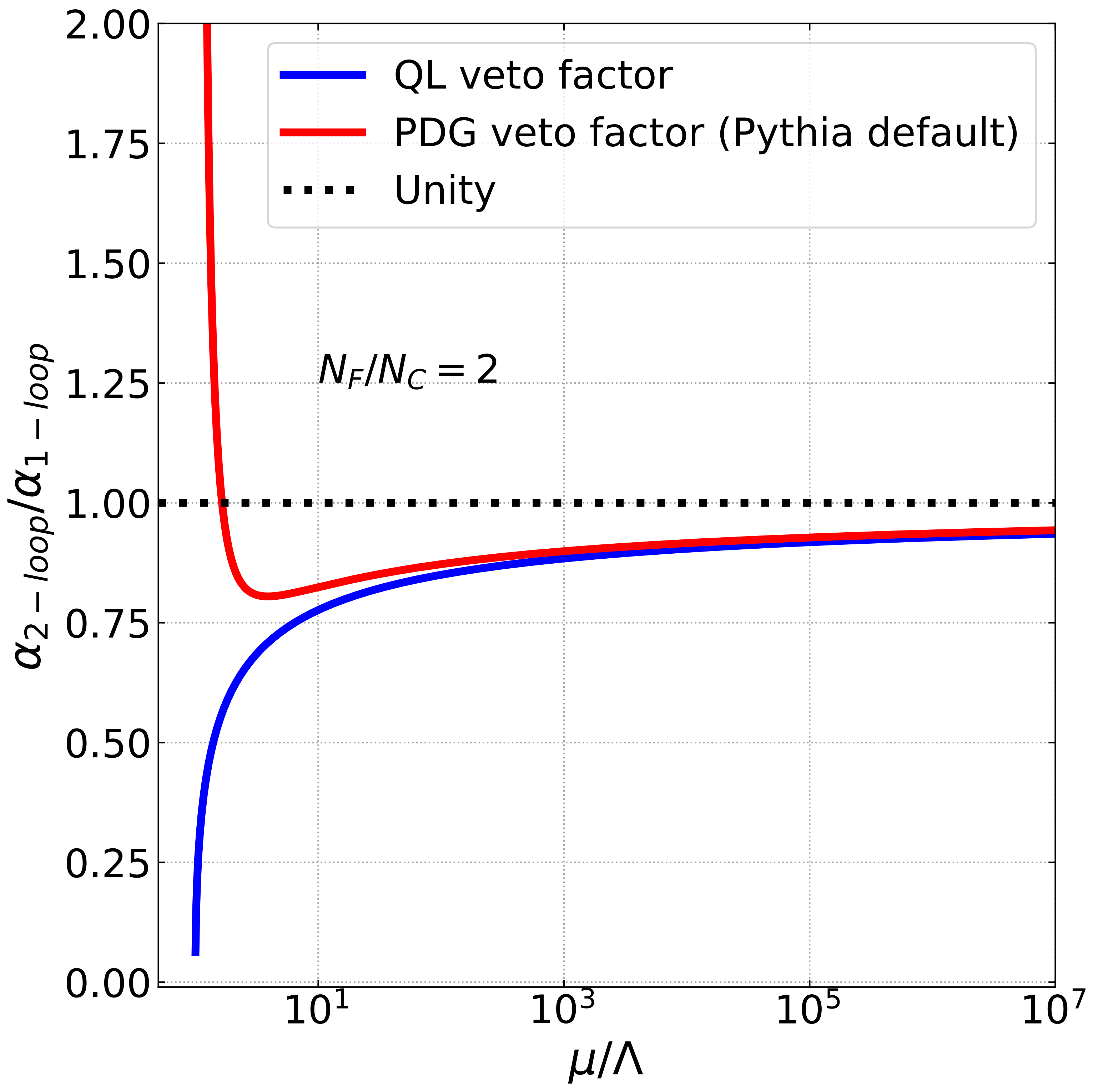

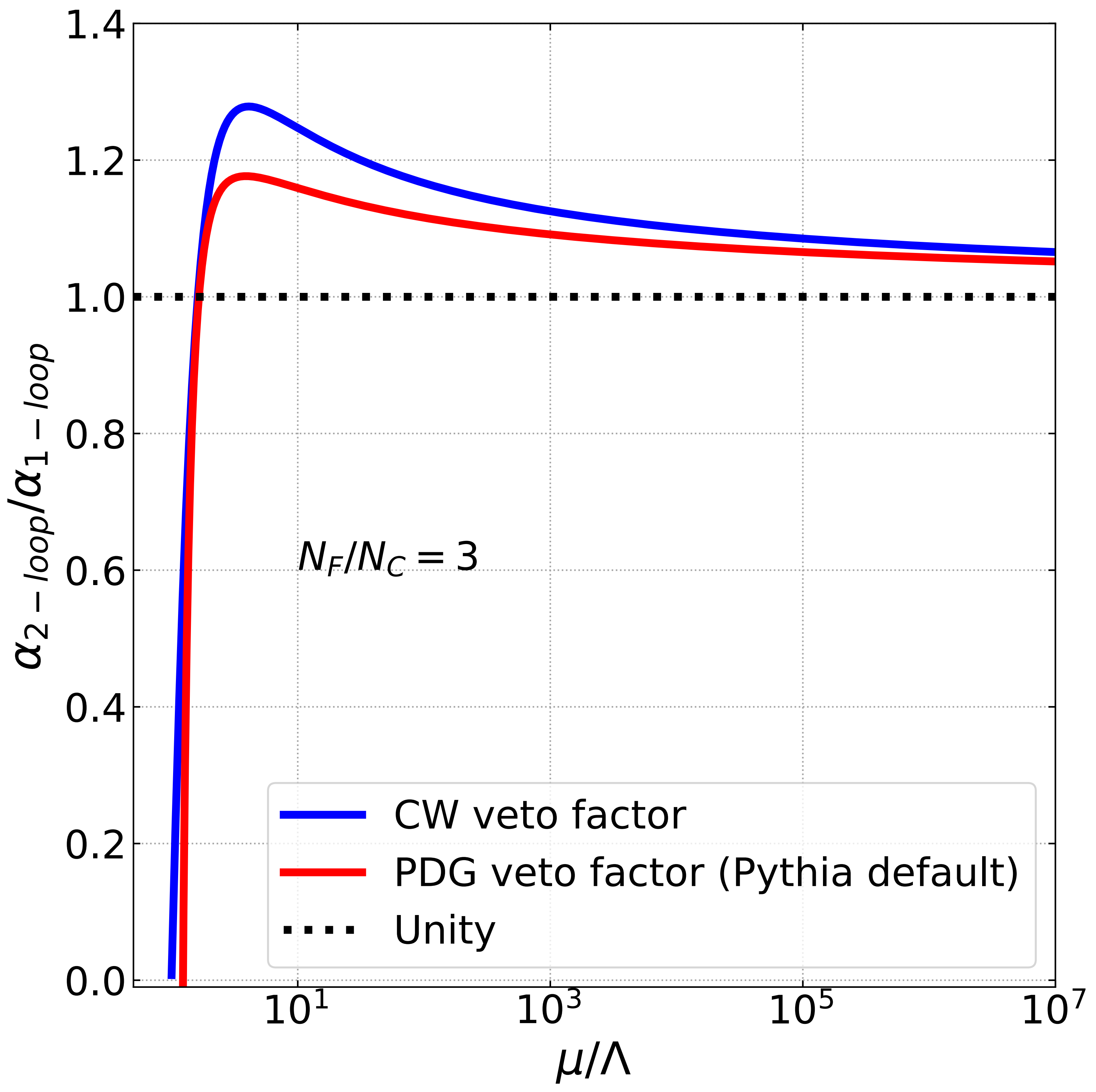

- To generate a scale Q_i^2 given an initial scale Q_{i-1}^2, event generators pick a random number R_1 and solve for $\Delta\left(Q_i^2, Q_{i-1}^2\right) = R_1$.
- Δ is the Sudakov factor, the probability of no parton emissions between Q_{i-1}^2 and Q_i^2 and serves to interface α and parton emission effects.

arXiv:0603175 - T. Sjöstrand et al.
arXiv:1102.2126 - W. Giele et al.
arXiv:1101.2599 - A. Buckley et al.
arXiv:1211.7204 - L. Lonnblad et al.

- Difficult to invert Δ, so usually invert a much simpler $\tilde{\Delta}$. Showering behaviour is then corrected for through the Sudakov veto algorithm. At two-loop, the inverse can be performed exactly with a LambertW function, implemented as before.
- Current Pythia two-loop efforts used another veto algorithm, instead of inverting, that additionally rejecting events with probability $\alpha_{2-loop}/\alpha_{1-loop}$, - a method not applicable for the entire N_F/N_C — μ/Λ space, especially the CW region.

Average dark parton multiplicity

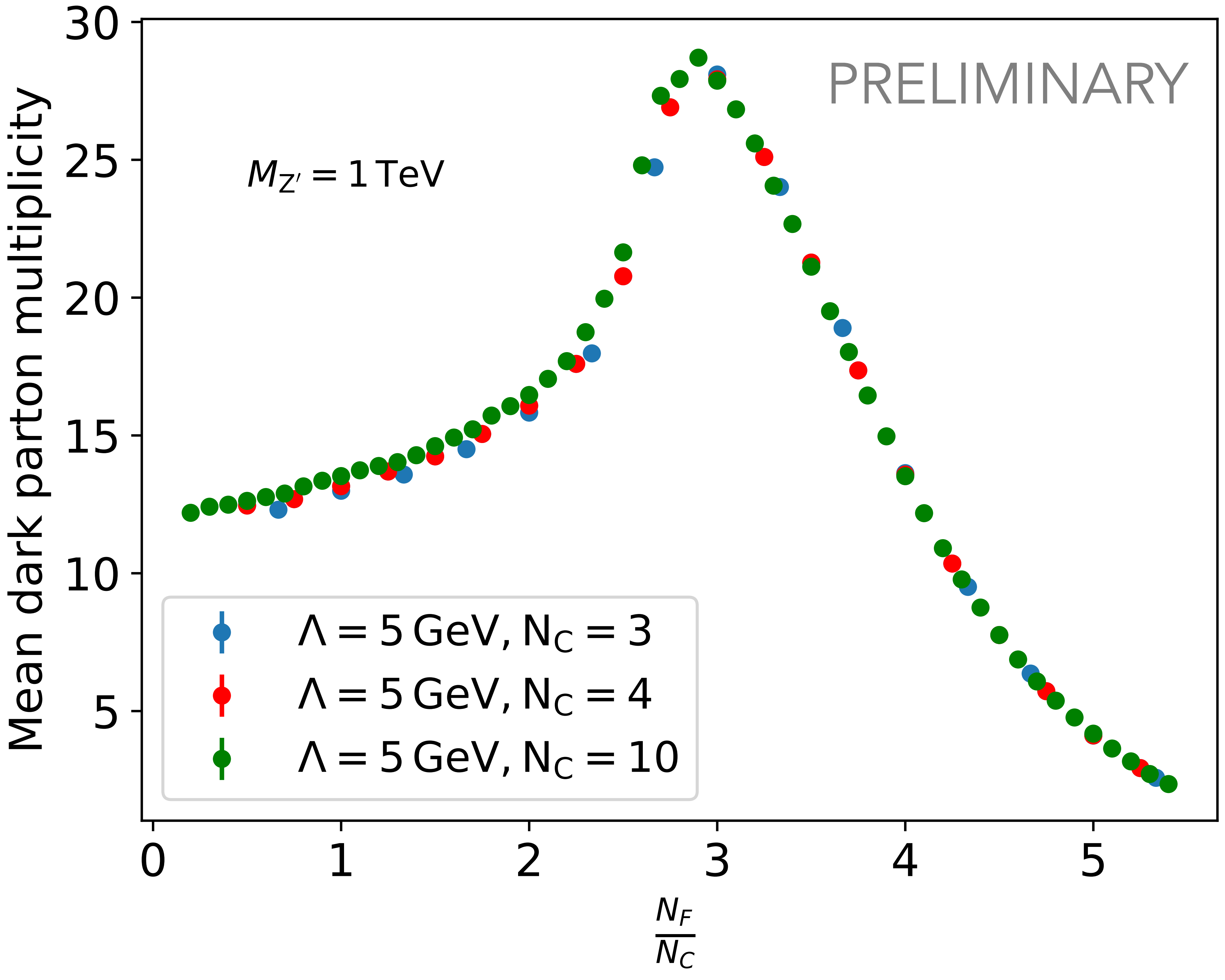

Simulated with a custom Pythia 8.307 with benchmark: $e^+e^- \to Z' \to q_D\overline{q_D}$, $\sqrt{s} = 1.1 M_{Z'} = 1.1$ TeV, hadronisation off , $\Lambda = 5$ GeV , $N_C = 3$. Cutoff at $Q = 1.1\Lambda$.

- Simulated using a custom version of Pythia 8.307; treat this implementation as a toy-model of near-conformal dark sectors. NOTE: we neglect the $P_{G_D \to q_D \bar{q}_D}$ branching - plan to add in future.
- Within the QL region, dark parton multiplicity increases with N_F/N_C. R. K. Ellis, W. J. Stirling and B. R. Webber, QCD and Collider Physics
- Theories with large IRFPs (around N_F/N_C ~3-4) have a large average multiplicity, which starts to decrease as $N_F/N_C \to 5.5$. Naively expect fat jets for large IRFPs and narrow (pencil-like) jets for N_F/N_C close to 5.5.
- The original PDG veto algorithm within Pythia can not predict this indicative rise and decreasing behaviour.

Average dark parton multiplicity

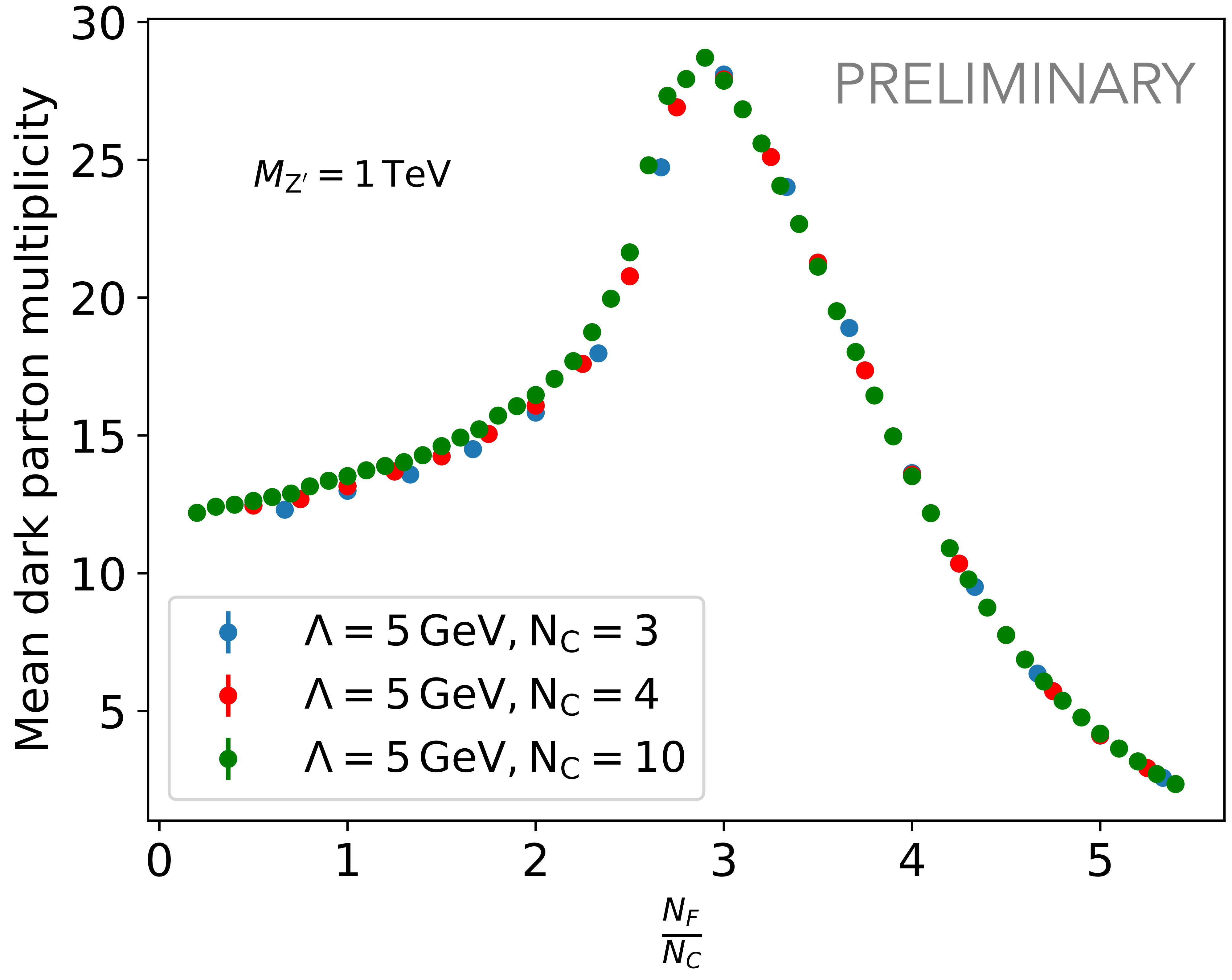

Simulated with a custom Pythia 8.307 with benchmark: $e^+e^- \to Z' \to q_D\overline{q_D}$, $\sqrt{s} = 1.1M_{Z'} = 1.1$ TeV, hadronisation off , $\Lambda = 5$ GeV , $N_C = 3$. Cutoff at $Q = 1.1\Lambda$.

- Parton splitting probability is proportional to α and vanishes as $N_F/N_C \to 5.5$. Parton splitting is unlikely at N_F/N_C ~ 5 and the average multiplicity tends to 2 - the 2 initial dark partons.

$$d\mathscr{P}_a\left(\xi, Q^2\right) = \frac{dQ^2}{Q^2}\frac{\alpha(Q^2)}{2\pi}\sum_{b,c} P_{a\to bc}(\xi)d\xi$$

- Need to validate this implementation by comparing jet multiplicities initiated by different partons i.e. $\langle N\rangle_{\text{gluon-jet}}$, $\langle N\rangle_{\text{quark-jet}}$. Then can move onto more complicated objects such as jet observables.

- This new procedure allows for the simulation of parton showers of near-conformal HV theories. Motivates further investigation into the hadronisation and decay of near-conformal bound states which also play a large role in dark shower phenomenology.

Thank you!
Questions?

Back-up

The zeroes of the β function

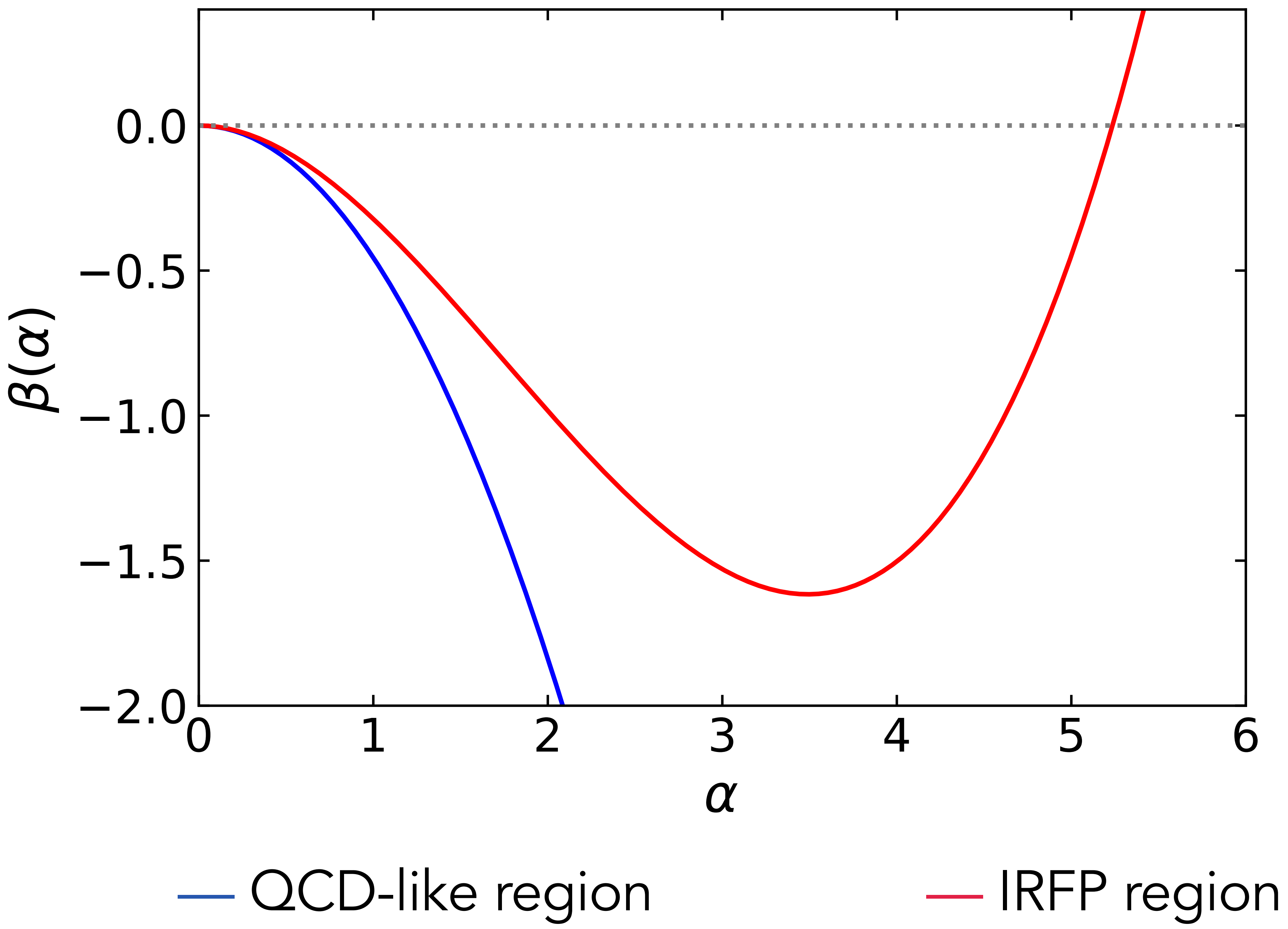

- The zeroes of the β function determine the UV and IR behaviour of the running coupling.

$$\beta(\alpha) = \mu^2 \frac{d\alpha}{d\mu^2} = -\alpha^2 \left(\beta_0 + \beta_1 \alpha\right)$$

- For $\beta_0 > 0$ ($N_F/N_C < 5.5$), the running coupling flows to $\alpha = 0$ in the UV - a trivial UV fixed point.

- At two-loop, there is also a zero at $\alpha_* = -\dfrac{\beta_0}{\beta_1}$. For $\beta_1 < 0$ ($N_F/N_C \gtrsim 2.7$), this is positive and so α flows to an interacting IR fixed point.

The conformal window?

- At some critical value $N_F/N_C = x_F^{crit.}$, chiral symmetry is restored and the running coupling of such massless conformal theories will flow toward an IRFP.

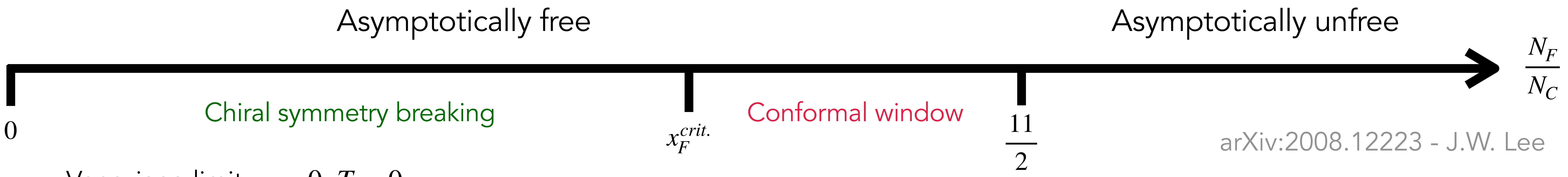

Veneziano limit, $\mu = 0$, $T = 0$

- Non-perturbative calculations place this critical number anywhere between $\frac{N_f}{N_c}$ = 3 - 4.

- Two-loop running coupling with IRFPs, which occur at $\frac{N_F}{N_C} \gtrsim 2.7$, provide a perturbative approximation of behaviour near the conformal window.

Fixed points and critical exponents

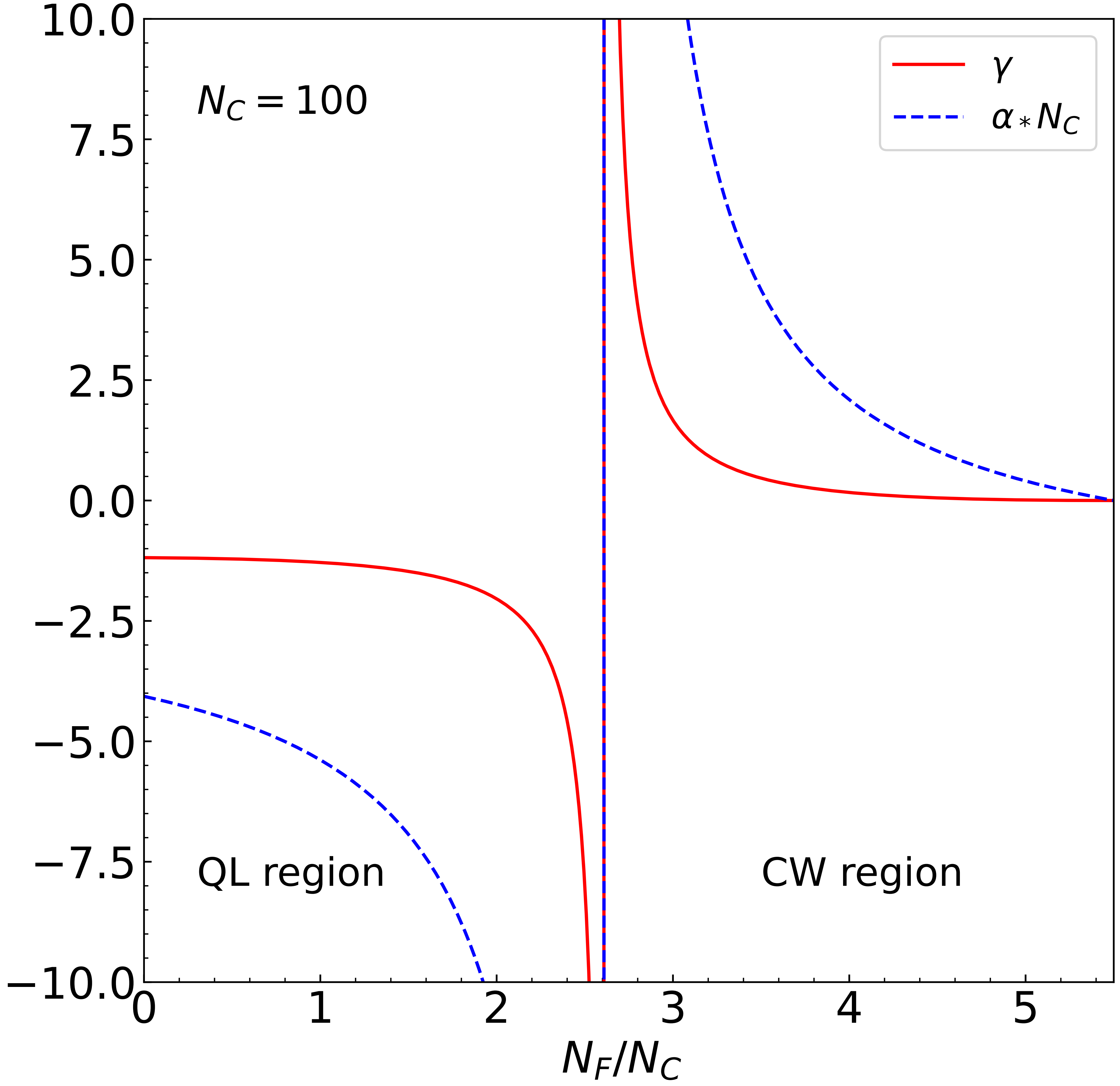

Large μ/Λ expansions

- For large μ/Λ, we have the following approximation in the QCD-like region,

$$\frac{1}{\alpha} = \beta_0 \ln\left(\frac{\mu^2}{\Lambda^2}\right) - \frac{1}{\alpha_*}\ln\left(1 - \beta_0\alpha_* \ln\left(\frac{\mu^2}{\Lambda^2}\right)\right) + \frac{1}{\alpha_*}\frac{\ln\left(1 - \beta_0\alpha_* \ln\left(\frac{\mu^2}{\Lambda^2}\right)\right)}{\beta_0\alpha_* \ln\left(\frac{\mu^2}{\Lambda^2}\right) - 1}$$

- This formula is valid to within the hadronisation cutoff of Pythia, unlike the PDG approximation.

- For large μ/Λ, we have the following approximation in the IRFP region,

$$\frac{1}{\alpha} = \beta_0 \ln\left(\frac{\mu^2}{\Lambda^2}\right) - \frac{1}{\alpha_*}\ln\left(\beta_0\alpha_* \ln\left(\frac{\mu^2}{\Lambda^2}\right) - 1\right) + \frac{1}{\alpha_*}\frac{\ln\left(\beta_0\alpha_* \ln\left(\frac{\mu^2}{\Lambda^2}\right) - 1\right)}{\beta_0\alpha_* \ln\left(\frac{\mu^2}{\Lambda^2}\right) - 1}$$

Running coupling - current procedure

- This problem could be avoided through assuming logarithmic terms dominate over the inverse of the magnitude of the IRFP. This gives the two-loop running coupling formula currently used by Pythia and the Particle Data Group (PDG),

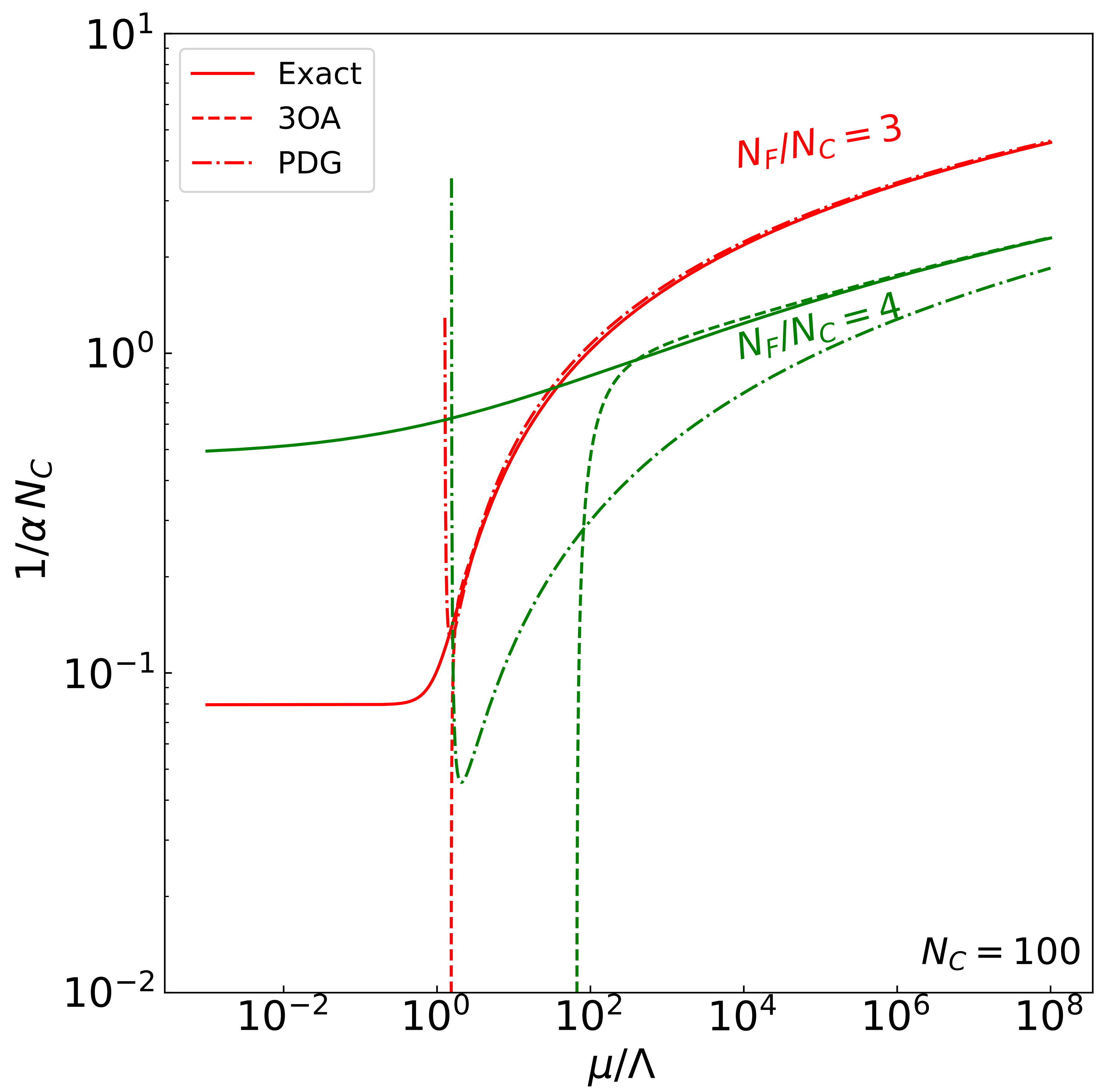

$$\frac{1}{\beta_0 \ln\left(\frac{\mu^2}{\Lambda^2}\right)} < |\alpha_*|$$

W.-M. Yao et al., Review of Particle Physics (2006) , arXiv:0607209, Prosperi et al.

$$\alpha = \frac{1}{\beta_0 \ln(\mu^2/\Lambda^2)}\left[1 + \frac{1}{\alpha_*}\frac{\ln[\ln(\mu^2/\Lambda^2)]}{\beta_0 \ln(\mu^2/\Lambda^2)}\right]$$

- For $N_F/N_C \gg (N_F/N_C)_*$, α_* becomes smaller, thus the PDG approximation begins to break down, inevitably leading to inaccurate showering behaviour.

- Thus the current approximation used within event generators (the PDG formula) is insufficient to describe two-loop α for high N_F/N_C since it neglects important effects of the IRFP.

New procedures for IRFPs

- We want a framework to define both α and Λ in regions with and without IRFPs. In general, perturbatively the scale Λ describes a cross-over between two scaling regions, below which the perturbative expansion breaks down. Our theory is weakly coupled in the UV ($\alpha(\mu_0) < \alpha_*$).
- The traditional definition of Λ remains within the QL region. Unlike the QL region, the low energy behaviour of running coupling in the CW region takes on a power-law form,

$$\alpha - \alpha_* \sim \left(\frac{\mu^2}{\mu_0^2}\right)^{\gamma} \quad ; \quad \gamma = \left.\frac{\partial \beta}{\partial \alpha}\right|_{\alpha=\alpha_*} = \beta_0 \alpha_* \qquad \text{(at 2-loop)}$$

- In the CW region, Λ is not the confinement scale, but rather characterises the crossover between power-law and logarithmic running behaviours. The exact scale below which the power-law dominates can be found to be,

$$\beta_0 \ln\left(\frac{\Lambda^2}{\mu_0^2}\right) = -\frac{1}{\alpha_0} - \frac{1}{\alpha_*}\ln\left(\frac{\alpha_*}{\alpha_0} - 1\right)$$

arxiv:9602385,

arxiv:9806409 - T. Appelquist et al.

arxiv:9810192 - E. Gardi et al.

Current approach for dark sector signatures

- Running coupling, α, determined by integrating the RGE.

Renormalisation Group Equation (RGE)

$$\mu^2 \frac{d\alpha}{d\mu^2} = \beta(\alpha)$$

$$= -\alpha^2 \left(\beta_0 + \beta_1 \alpha\right) \quad \text{(at two-loop)}$$

Integrate assuming $\frac{1}{\beta_0 \ln\left(\frac{\mu^2}{\Lambda^2}\right)} \gg |\alpha_*|$ → Approximate running coupling implemented in Pythia.

Equivalent at one-loop order, but not higher orders.

Integrate to obtain implicit solution → "Exact" running coupling needed to understand infra-red properties.

- Λ is defined to be the scale where the α diverges; below this scale the perturbative expansion in terms of the RGE is not reliable. For SM QCD, Λ_{QCD} is a useful proxy for the scale of the theory.
- Current approximation methods by definition ignore the contributions of the IRFP.

The PDG approximation

- Starting from the two-loop exact QCD-like solution for the running coupling,

$$\alpha = \alpha_* \left[W_{-1}\left(-\frac{1}{e}\left(\frac{\mu^2}{\Lambda^2}\right)^{\beta_0\alpha_*} \right) + 1 \right]^{-1}$$

- We can perform an expansion for large μ/Λ as before but under the assumption that,

$$\frac{1}{\beta_0 \ln(\mu^2/\Lambda^2)} \ll |\alpha_*|$$

- This assumption gives the following form of the PDG approximation.

$$\alpha(\mu^2) = \frac{1}{\beta_0 \ln(\mu^2/\Lambda^2)}\left(1 - \frac{\beta_1}{\beta_0^2}\frac{\ln(\ln(\mu^2/\Lambda^2))}{\ln(\mu^2/\Lambda^2)}\right)$$

- Since this neglects effects of the IRFP and is an expansion in large μ/Λ, it clearly cannot capture the effects of the IRFP.

Defining a scale in the IRFP region

- In general, the scale Λ describes a cross-over between two regions, below which perturbative expansion is invalid. Unlike the QCD-like region, the low energy behaviour of running in the IRFP region takes on a power-law form,

$$\alpha - \alpha_* \sim \left(\frac{\mu^2}{\mu_0^2}\right)^{\beta_0 \alpha_*}$$

- IRFP region α runs slower, but still displays asymptotically free logarithmic behaviour at high energies.

- In the IRFP region, we can define Λ as the transition between the asymptotic free $\sim \frac{1}{log}$ and power-law behaviour. The exact scale below which the power-law dominates can be found to be,

$$\beta_0 \ln\left(\frac{\Lambda^2}{\mu_0^2}\right) = -\frac{1}{\alpha_0} - \frac{1}{\alpha_*}\ln\left(\frac{\alpha_*}{\alpha_0} - 1\right)$$

arXiv:9602385,

arXiv:9806409 - T. Appelquist et al.

arXiv:9810192 - E. Gardi et al.

New procedures for IRFPs

- By taking this IRFP into account, we establish a framework of two solutions to the RGE that accurately describe the running coupling in regions with and without IRFPs.

- From this, we can find the explicit forms in both regions in terms of the two real branches of the Lambert W function,

$$\alpha = \alpha_* \left[W_{-1}(-z) + 1\right]^{-1} \quad ; \quad \alpha = \alpha_* \left[W_0(z) + 1\right]^{-1} \quad ; \quad z = \frac{1}{e}\left(\frac{\mu^2}{\Lambda^2}\right)^{\beta_0 \alpha_*}$$

QCD-like (QL)-region

"Conformal window" (CW)-region

- For large μ/Λ, we can use the third order expansion (3OA) in both branches of the Lambert W function of,

$$W(x) = L_1 - L_2 + \frac{L_2}{L_1} + \mathcal{O}\left(\left[\frac{L_2}{L_1}\right]^2\right)$$

- Where $L_1 = \ln(z)$, $L_2 = \ln\left(\ln(z)\right)$ for $W_0(z)$ and $L_1 = \ln(z)$, $L_2 = \ln\left(-\ln(z)\right)$ for $W_{-1}(-z)$,

New procedures for IRFPs

- By expanding for large μ/Λ, we obtain closed-form UV expansions of our two solutions. This gives the following third order expansion in the QL region of,

$$\frac{1}{\alpha} = \beta_0 \ln\left(\frac{\mu^2}{\Lambda^2}\right) - \frac{1}{\alpha_*}\ln\left(1 - \beta_0\alpha_* \ln\left(\frac{\mu^2}{\Lambda^2}\right)\right) + \frac{1}{\alpha_*}\frac{\ln\left(1 - \beta_0\alpha_*\ln\left(\frac{\mu^2}{\Lambda^2}\right)\right)}{\beta_0\alpha_*\ln\left(\frac{\mu^2}{\Lambda^2}\right) - 1}$$

QL approximation

- And in the CW region of,

$$\frac{1}{\alpha} = \beta_0 \ln\left(\frac{\mu^2}{\Lambda^2}\right) - \frac{1}{\alpha_*}\ln\left(\beta_0\alpha_* \ln\left(\frac{\mu^2}{\Lambda^2}\right) - 1\right) + \frac{1}{\alpha_*}\frac{\ln\left(\beta_0\alpha_*\ln\left(\frac{\mu^2}{\Lambda^2}\right) - 1\right)}{\beta_0\alpha_*\ln\left(\frac{\mu^2}{\Lambda^2}\right) - 1}$$

CW approximation

Monte Carlo implementation

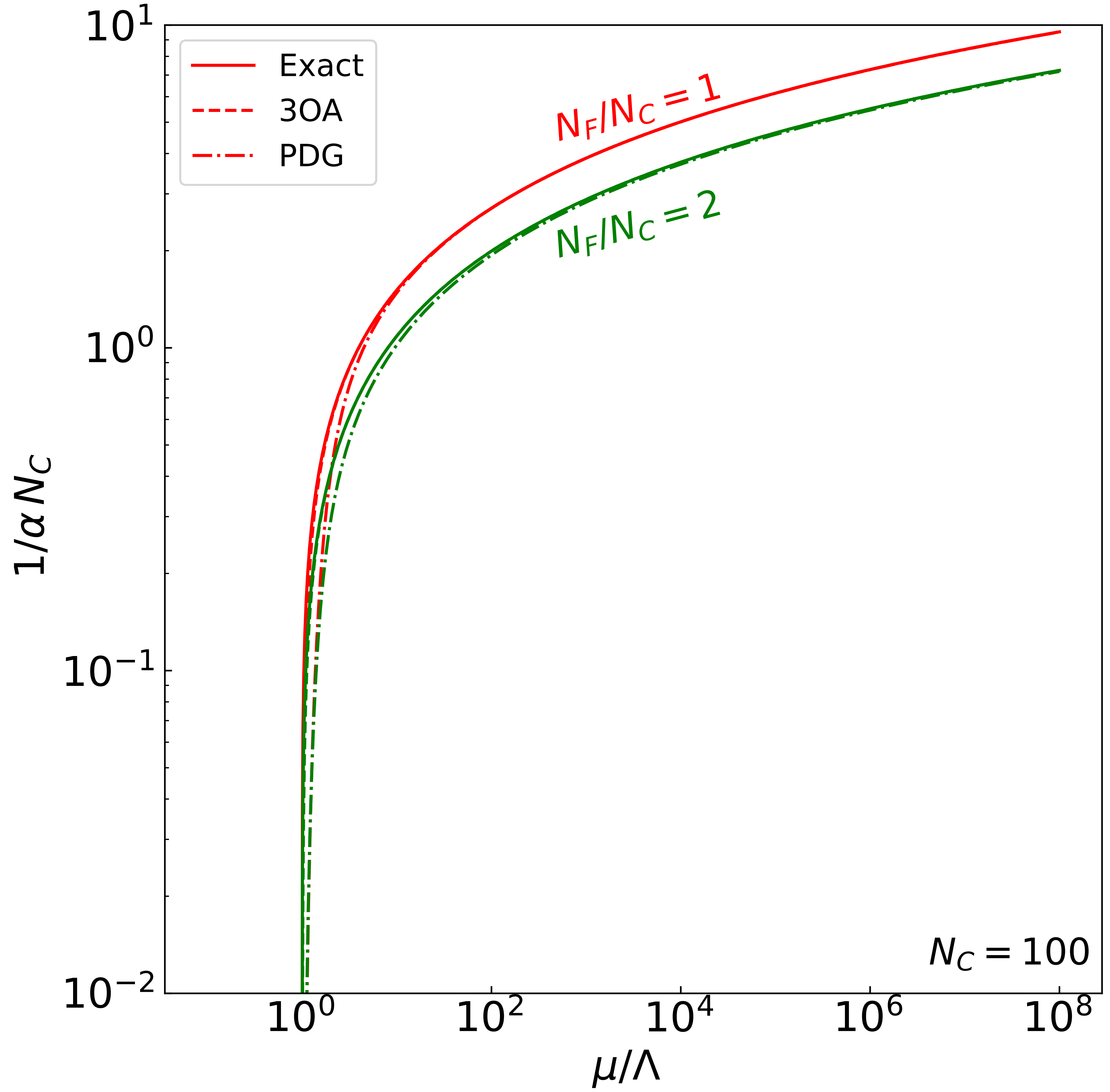

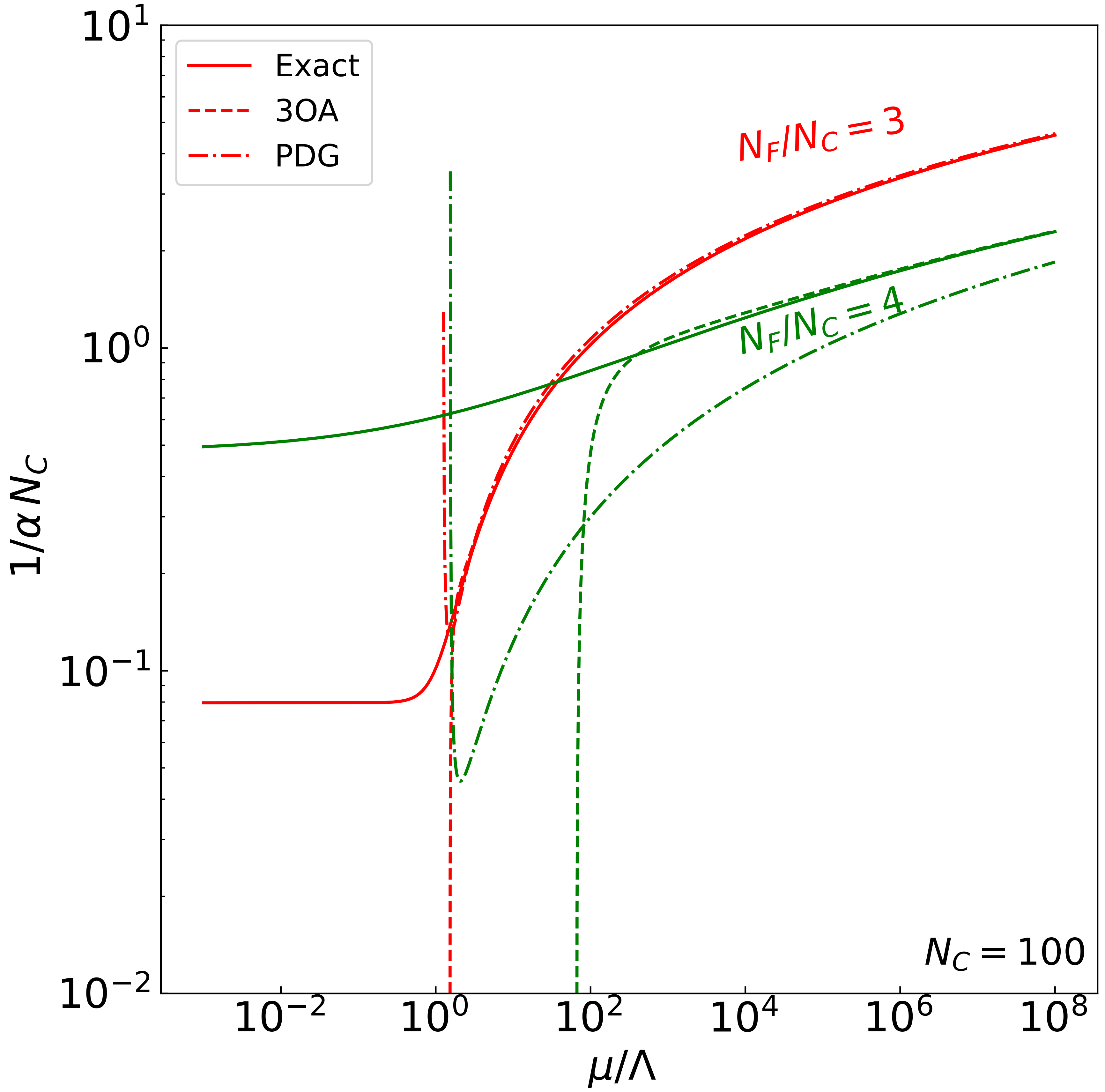

- The CW 3OA approximation covers more of $N_F/N_C - \mu/\Lambda$ space than the PDG approximation, providing the best approximation when $N_F/N_C \sim (N_F/N_C)_*$. However, increasing N_F/N_C close to 4, the energy range over which the CW approximation proves to be reliable begins to decrease, however is still accurate within the UV.

Monte Carlo implementation

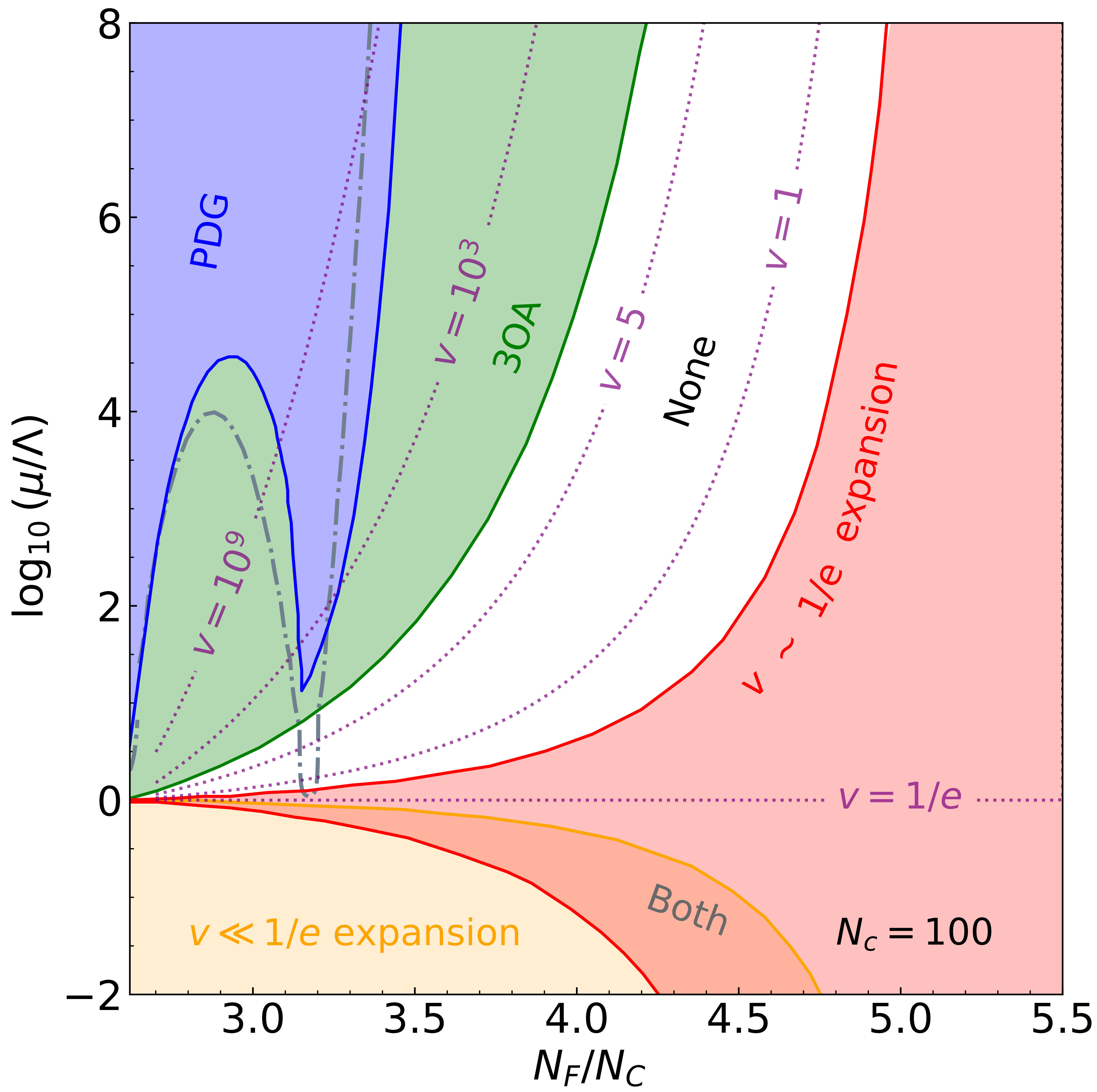

- A full comparison of the validity (deviation by over 2%) of the CW and PDG approximations in $N_F/N_C - \mu/\Lambda$ space reveals a large area of parameter space covered by neither.
- Various IR expansions were considered, e.g. expanding the exact CW solution around $z = 0$ or $z = 1/e$ but none could provide full coverage over all parameter space.
- Since the running of the coupling within the uncovered region is so slow, interpolating the "exact" CW solution was found to be the most reliable approximation within this region.

Validity in the QL region

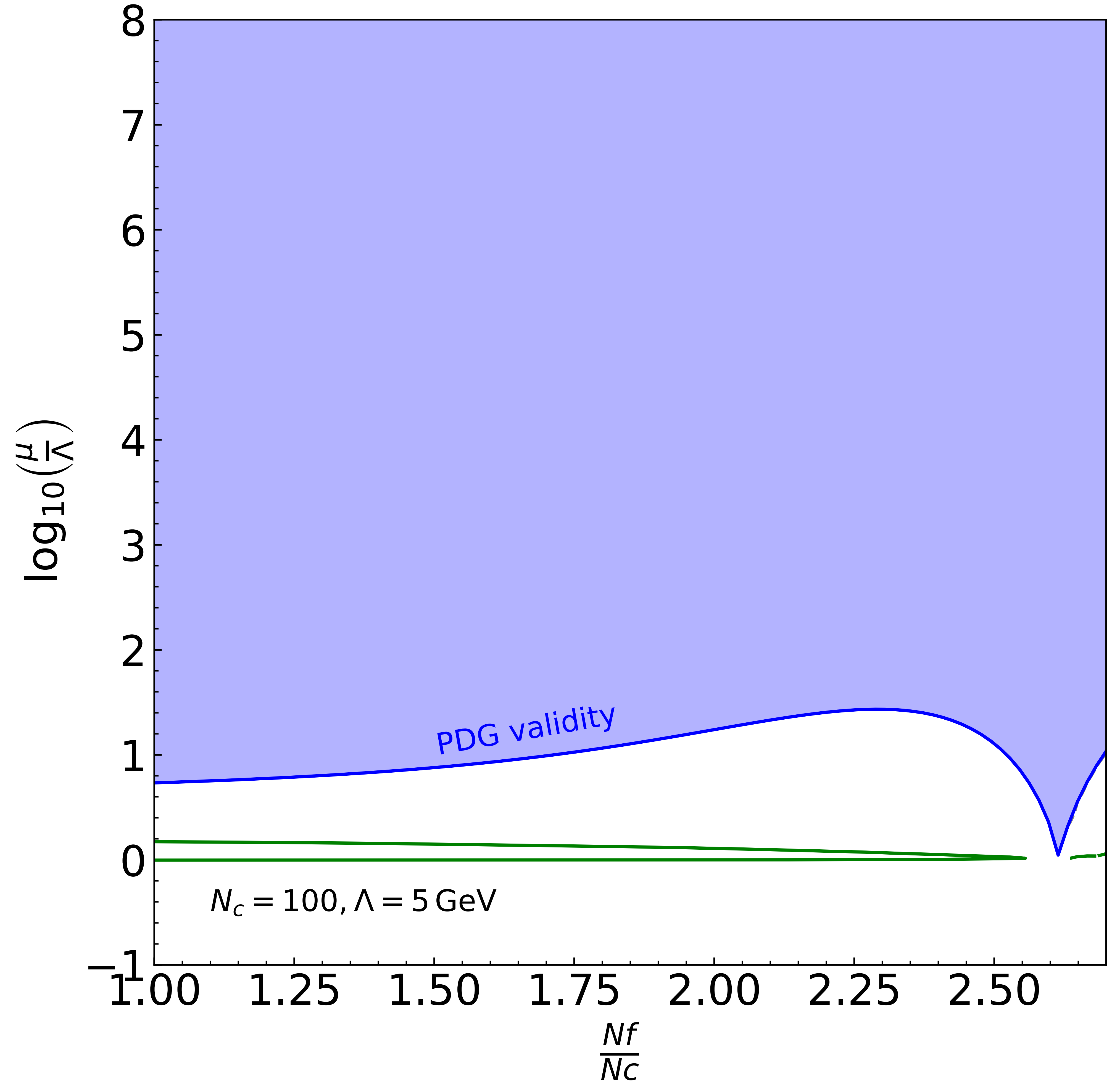

Interpolation procedure

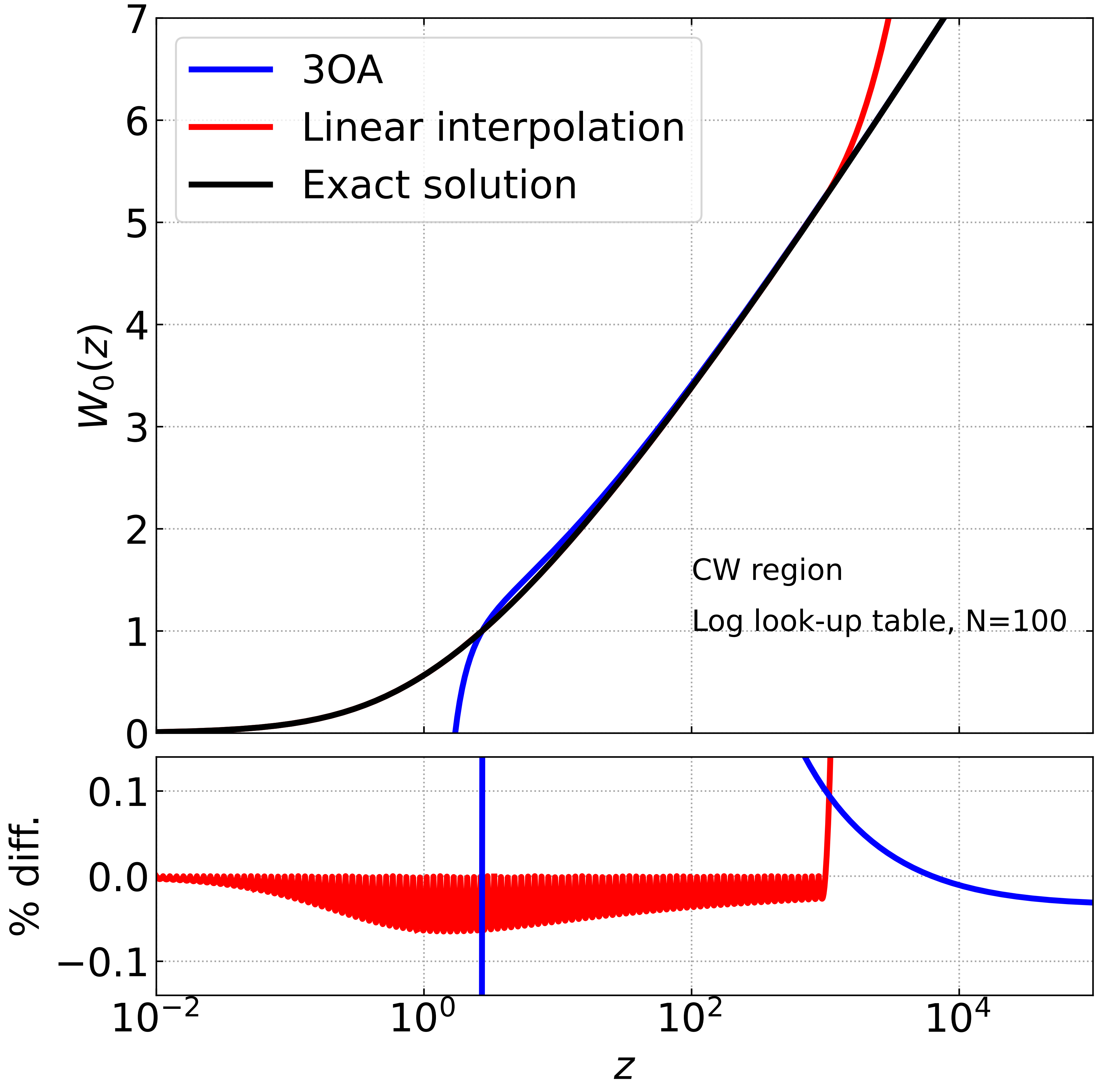

- Within the QL region, the implementation of the running coupling suffices with a large μ/Λ approximation (3OA) for all $\mu/\Lambda > 1$.

- The 3OA fails in the CW region when the running coupling is slow - an area that lends itself nicely to interpolation. The best solution was to use a 3OA where applicable and linearly interpolate the regions where it fails.

- It is convenient to interpolate in z space; taken over z between a range of 10^{-2} and 10^{3} using 100 data points. The upper boundary of this interpolation is determined by when the large μ/Λ approximation deviates from the exact solution by 0.1%.

Implementing running coupling

- The Sudakov form factor is another important ingredient in the modelling the final state radiation of the parton shower. It is the probability of no parton emissions between two scales; the initial scale Q_1^2 and the scale of the next emission Q_2^2. The Sudakov factor of parton, a, splitting into partons b and c is given by,

$$\Delta_a = \exp\left(-\int_{Q_1^2}^{Q_2^2} \frac{dQ'^2}{Q'^2} \int_{\xi_{min}(Q'^2)}^{\xi_{max}(Q'^2)} \frac{\alpha}{2\pi} P_{a\to bc}(\xi')d\xi' \right)$$

arxiv:1102.2126 - W. Giele et al.

R. Ellis, W. Stirling, B. Webber

- Where ξ is the fraction of energy given to b; it governs the longitudinal evolution of the parton shower. $P_{a\to bc}$ are the Altarelli-Parisi splitting functions. Parton shower splitting functions can be expressed in terms of Casimir invariants and ξ,

$$P_{G_D\to G_D G_D} = C_A \frac{1+\xi^3}{1-\xi}; \quad P_{q_D\to q_D G_D} = \frac{1}{2} C_F \frac{1+\xi^2}{1-\xi}; \quad P_{G_D\to q_D \bar{q}_D} = T_R \left(\xi^2 + (1-\xi)^2\right)$$

- In event generators, at every step of parton splitting, we want to generate a new set of $\left[Q_i^2, \xi_i\right]$ (focus only on Q_i^2 for now). Given some initial scale Q_2^2, we can sample Q_1^2 by generating a random number R_1 between 0 and 1 and solving $\Delta\left(Q_1^2, Q_2^2\right) = R_1$. We can use the veto algorithm to solve this!

Two-loop veto algorithm

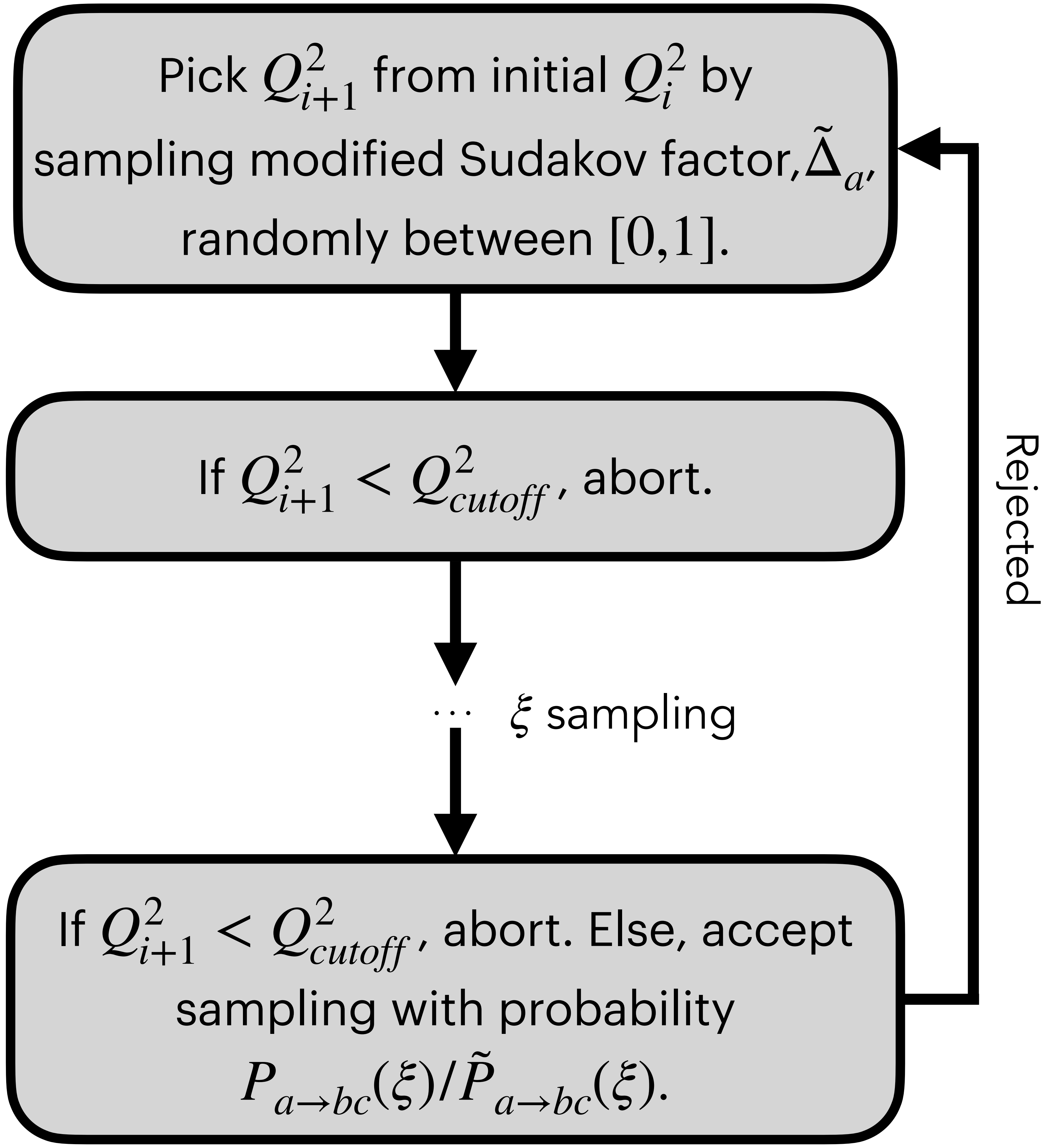

- Inverting the Sudakov factor is not always possible. Instead we overestimate the tree-level splitting functions by some $\tilde{P}_{a\to bc}(\xi')$.

$$\tilde{P}_{G_D\to G_D G_D} = 2C_A\frac{1}{1-\xi}; \quad \tilde{P}_{q_D\to q_D G_D} = C_F\frac{1}{1-\xi}; \quad \tilde{P}_{G_D\to q_D\bar{q}_D} = T_R$$

- We also overestimate the integration region with boundaries independent of Q^2 : $\tilde{\xi}_{max}({Q_0}^2) > \xi_{max}(Q'^2)$ and $\tilde{\xi}_{min}({Q_0}^2) < \xi_{min}(Q'^2)$.
- At one-loop, we can now write a closed-form expression in terms of the modified Sudakov factor, $\tilde{\Delta}_a$.

$$\ln(Q_2^2/\Lambda^2) = \tilde{\Delta}_a^{2\pi\beta_0/\epsilon_a}\ln(Q_1^2/\Lambda^2); \quad \epsilon_a = \int_{\tilde{\xi}_{min}}^{\tilde{\xi}_{max}} \sum_{b,c} \tilde{P}_{a\to bc}(\xi')d\xi';$$

ϵ_a is the "emission coefficient"

- Overestimating can be corrected for by rejecting each event with probability $P_{a\to bc}/\tilde{P}_{a\to bc}$.

arXiv:0603175 - T. Sjöstrand et al. arXiv:1101.2599 - A. Buckley et al. arXiv:1211.7204 - L. Lonnblad et al.

Two-loop veto algorithm

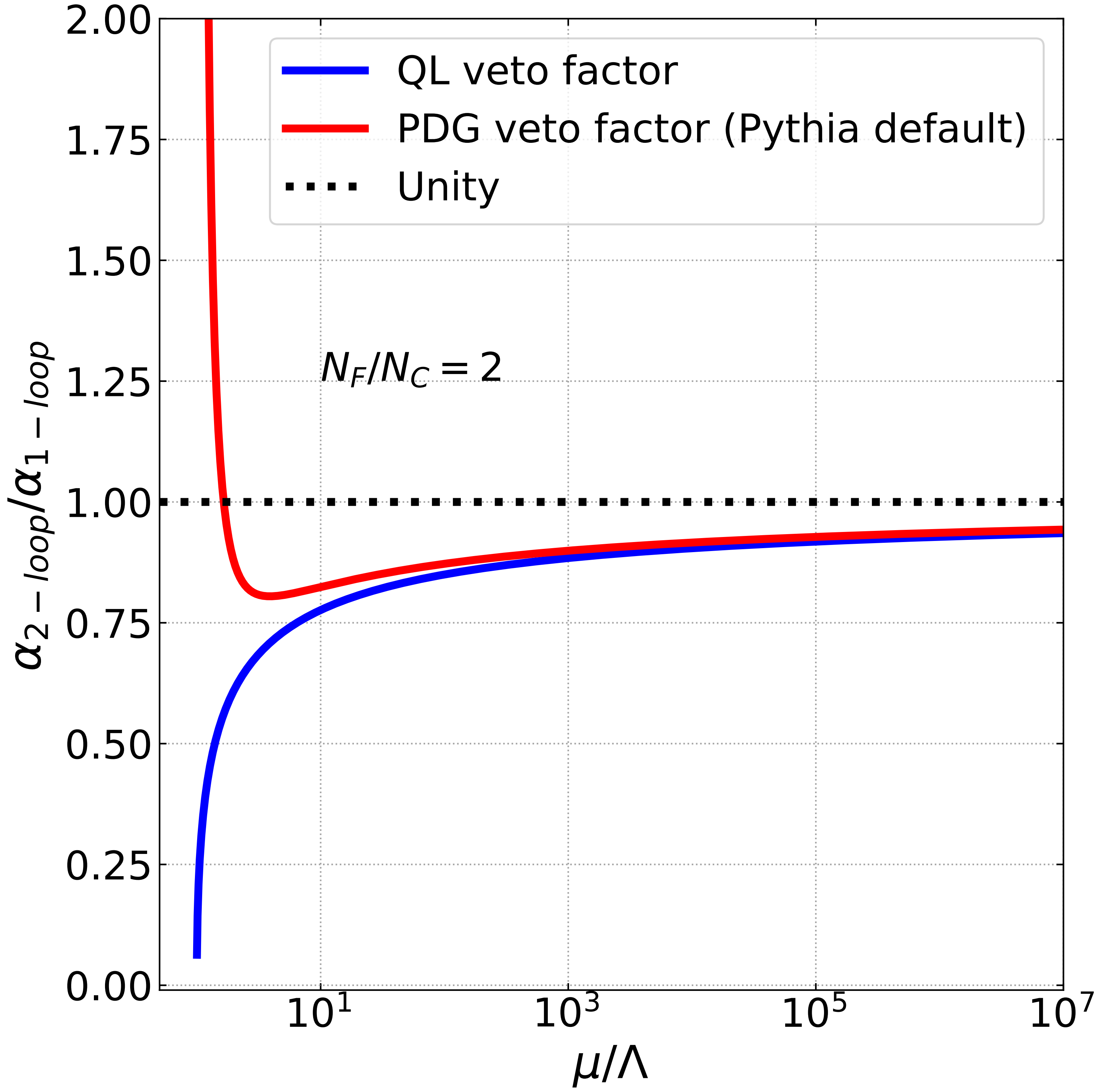

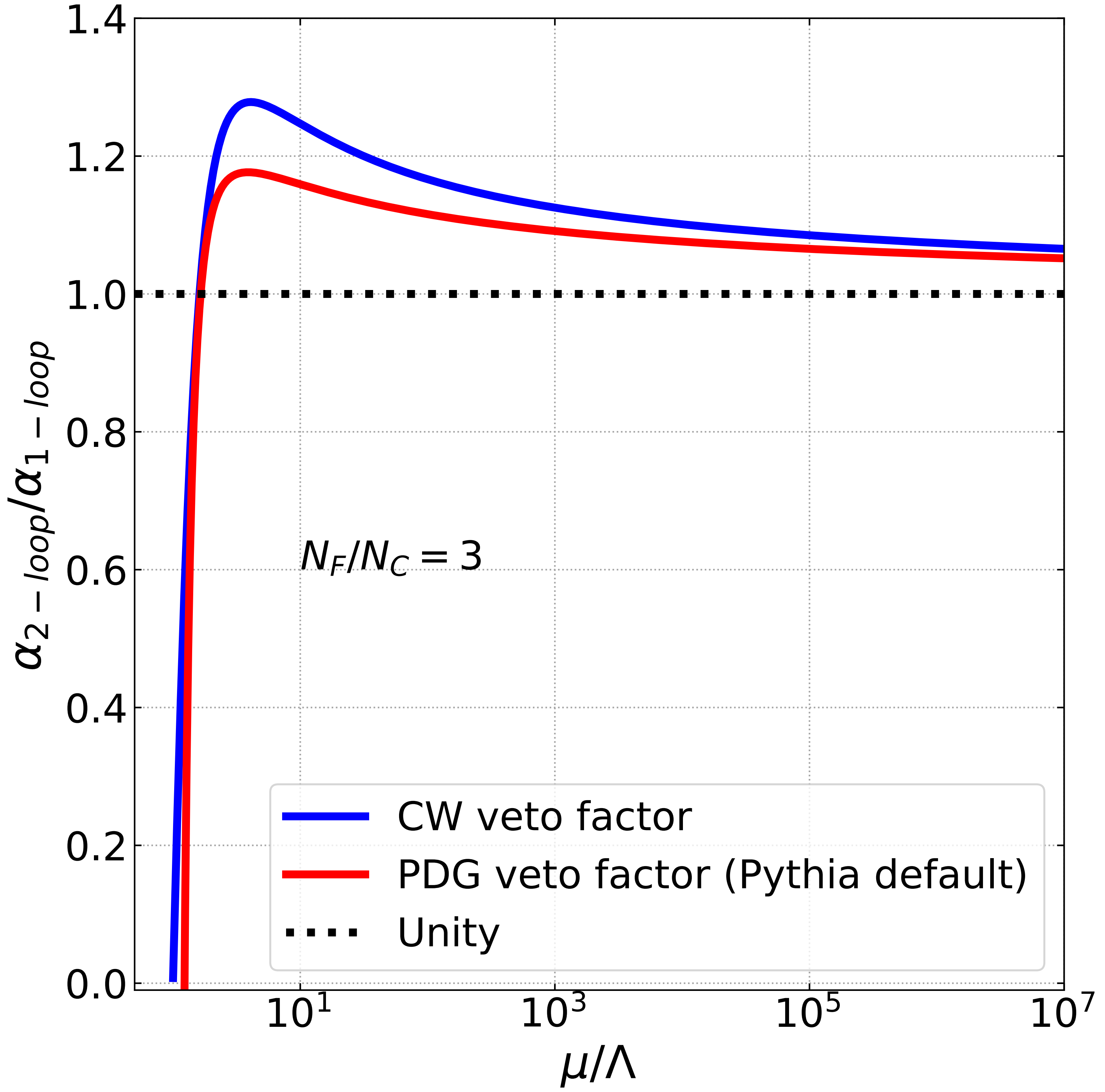

Pick Q^2_{i+1} from initial Q^2_i by sampling modified Sudakov factor, $\tilde{\Delta}_{a'}$ randomly between $[0,1]$.

For two-loop, overestimate α_{2-loop} with α_{1-loop} and accept sampling with probability $\alpha_{2-loop}/\alpha_{1-loop}$.

If $Q^2_{i+1} < Q^2_{cutoff}$, abort.

- Since the exact running coupling is given in terms of a special function, this contributes an additional difficulty in inverting the Sudakov factor.
- Current Pythia two-loop efforts used another veto algorithm that additionally rejecting events with probability $\alpha_{2-loop}/\alpha_{1-loop}$, - a method not applicable for the entire N_F/N_C — μ/Λ space, especially the CW region.

An improved Sudakov veto algorithm

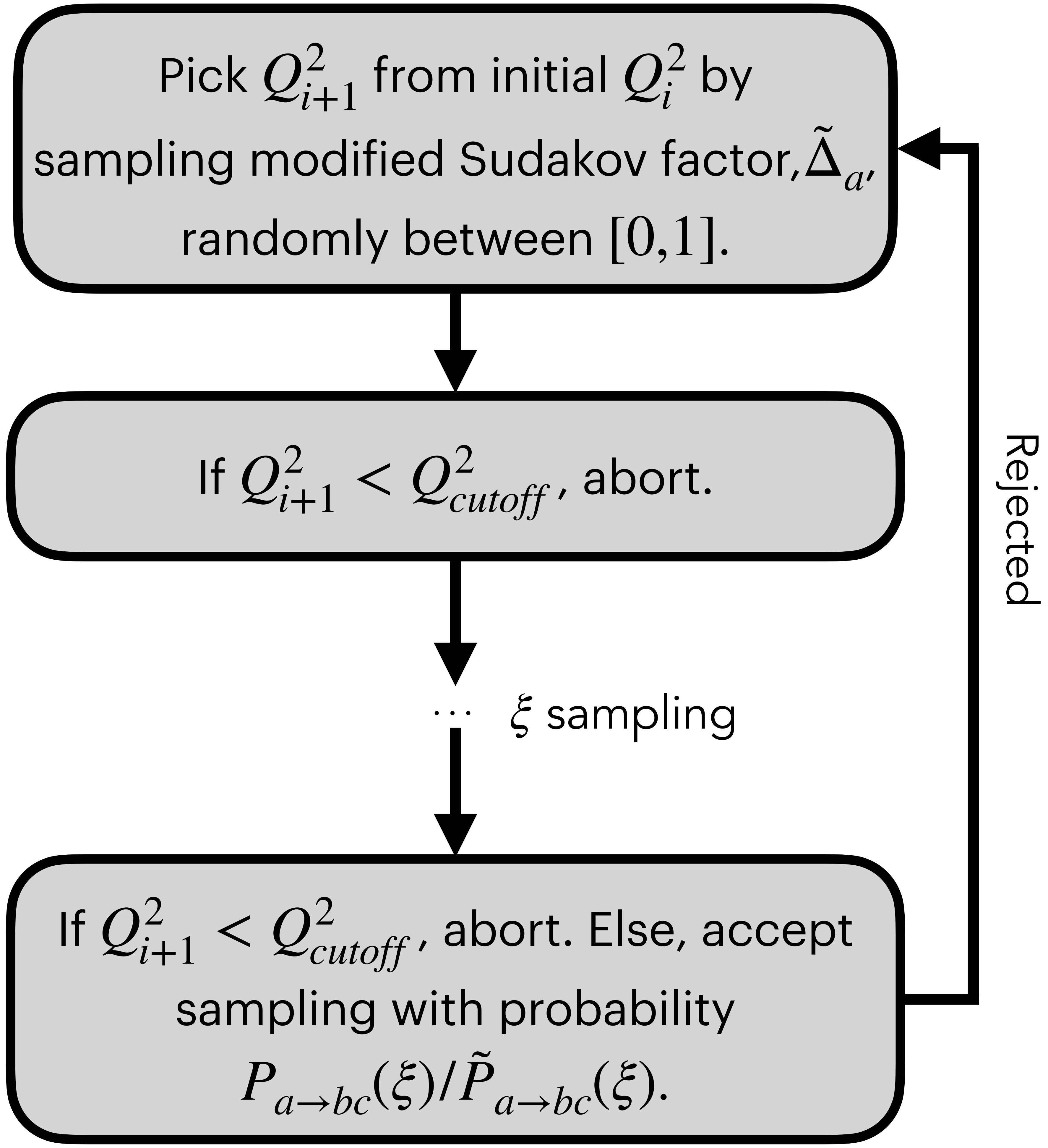

- Can calculate an inverse at two-loop using overestimated splitting functions, no need for any α veto algorithm/ overestimates.

QL region
$$Q_2^2 = \Lambda^2 \left(\frac{Q_1^2}{\Lambda^2}\right)^{\tilde{\Delta}_a^{2\pi\beta_0/\epsilon}} \left[\tilde{\Delta}_a^{2\pi\beta_0/\epsilon}\left(-eW_{-1}(-z_1)\right)^{1-\tilde{\Delta}_a^{2\pi\beta_0/\epsilon}}\right]^{1/\gamma}$$

CW region
$$Q_2^2 = \Lambda^2 \left(\frac{Q_1^2}{\Lambda^2}\right)^{\tilde{\Delta}_a^{2\pi\beta_0/\epsilon}} \left[\tilde{\Delta}_a^{2\pi\beta_0/\epsilon}\left(eW_{0}(z_1)\right)^{1-\tilde{\Delta}_a^{2\pi\beta_0/\epsilon}}\right]^{1/\gamma}$$

$$z_1 = z\Big|_{Q=Q_1}$$

- Since LambertW is not in Pythia, have to implement approximations and interpolations. For large μ/Λ, we use a third order expansion (3OA) in both branches of the Lambert W function,

$$W_{-1/0}(\mp z) = \ln(z) - \ln\left(\mp\left(\ln(z)\right)\right) + \frac{\ln\left(\mp\left(\ln(z)\right)\right)}{\ln(z)} \quad ; \quad \mp = \begin{cases} - & \text{(QL)} \\ + & \text{(CW)} \end{cases}$$

- For the QL region, we can simply use the large μ/Λ expansion.

arXiv:0603175 - T. Sjöstrand et al. arXiv:1101.2599 - A. Buckley et al. arXiv:1211.7204 - L. Lonnblad et al.

Setup, caveats, future progress

- Simulated within a custom version of Pythia 8.307. We treat this implementation as a toy-model of near-conformal dark sectors and hence describe the qualitative behaviour of near-conformal dark parton showers and is not quantitive.
- As such, we neglect the $P_{G_D \to q_D \bar{q}_D}$ branching, as is standard within the Hidden Valley module of Pythia. Additionally, we neglect any implementation of a CMW scheme change. S. Catani, B. R. Webber, G. Marchesini, Nucl. Phys. B 349 ('91)
- In fact, we have working implementations of both of these, but await validation before discussing the phenomenology. To implement the $P_{G_D \to q_D \bar{q}_D}$ branching we have to calculate the individual emission coefficients for the process $G_D \to b, c$:

$$\epsilon_a = \sum_{b,c} \epsilon_{a \to bc} \quad ; \quad \epsilon_{G_D \to q_D \bar{q}_D} = T_R \left(1 - 2\tilde{\xi}_{min}\right) \quad ; \quad \epsilon_{G_D \to G_D G_D} = C_A \ln\left(\frac{1}{\tilde{\xi}_{min}} - 1\right)$$

- Therefore the branching of $G_D \to q_D \bar{q}_D$ is chosen with probability $\epsilon_{G_D \to q_D \bar{q}_D} / \epsilon_a$ during the parton showering process.

Average dark parton multiplicity

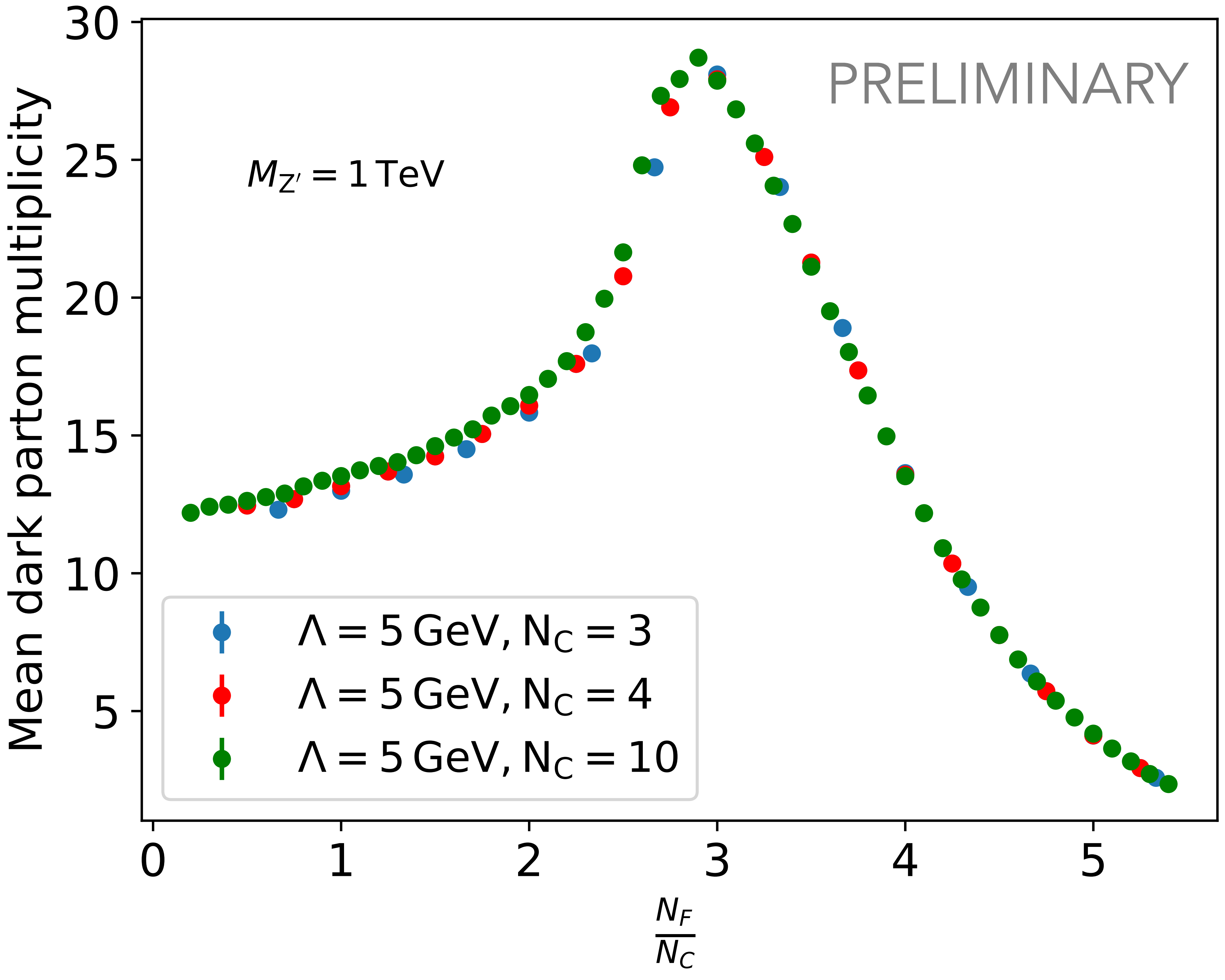

Simulated with a custom Pythia 8.307 with benchmark: $e^+e^- \to Z' \to q_D\overline{q_D}$, $\sqrt{s} = 1.1M_{Z'} = 1.1$ TeV, hadronisation off , $\Lambda = 5$ GeV , $N_C = 3$. Cutoff at $Q = 1.1\Lambda$.

- Within the QL region, dark parton multiplicity increases with N_F/N_C. R. K. Ellis, W. J. Stirling and B. R. Webber, QCD and Collider Physics
- Theories with large IRFPs (around N_F/N_C ~3) have a large average multiplicity. The multiplicity trend reverses at N_F/N_C just above $(N_F/N_C)_*$. Hence, theories with small IRFPs (around N_F/N_C ~5) have a small average multiplicity.
- Parton splitting probability is proportional to α and vanishes as $N_F/N_C \to 5.5$. Parton splitting is unlikely at $N_F/N_C \sim 5$ and the average multiplicity tends to 2 - the 2 initial dark quarks.

$$d\mathscr{P}_a\left(\xi, Q^2\right) = \frac{dQ^2}{Q^2}\frac{\alpha(Q^2)}{2\pi}\sum_{b,c} P_{a\to bc}(\xi)d\xi$$

- The original PDG veto algorithm within Pythia can not predict this indicative decreasing behaviour.

Simulation of dark parton showers

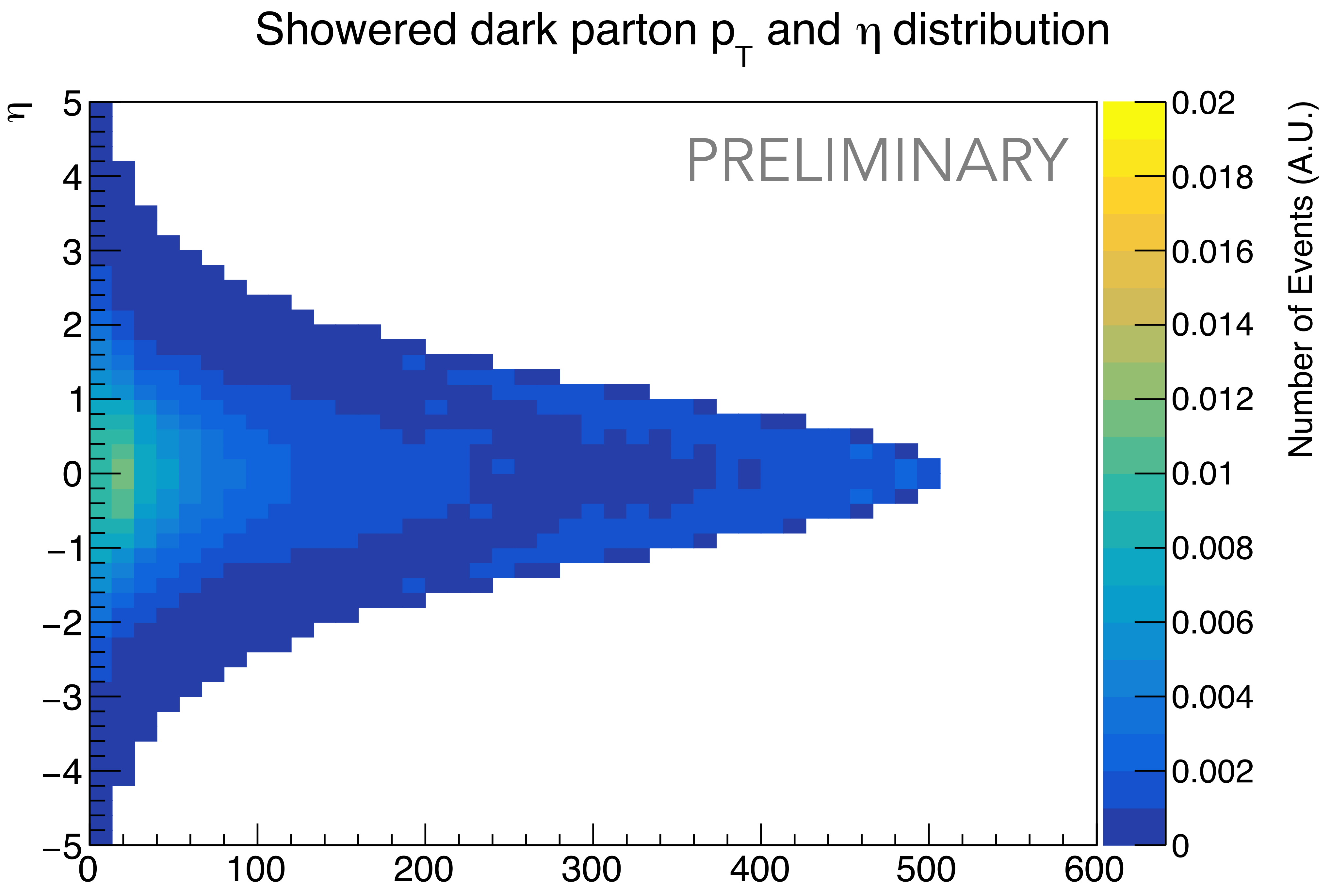

$\Lambda = 5$ GeV , $N_F = 14$

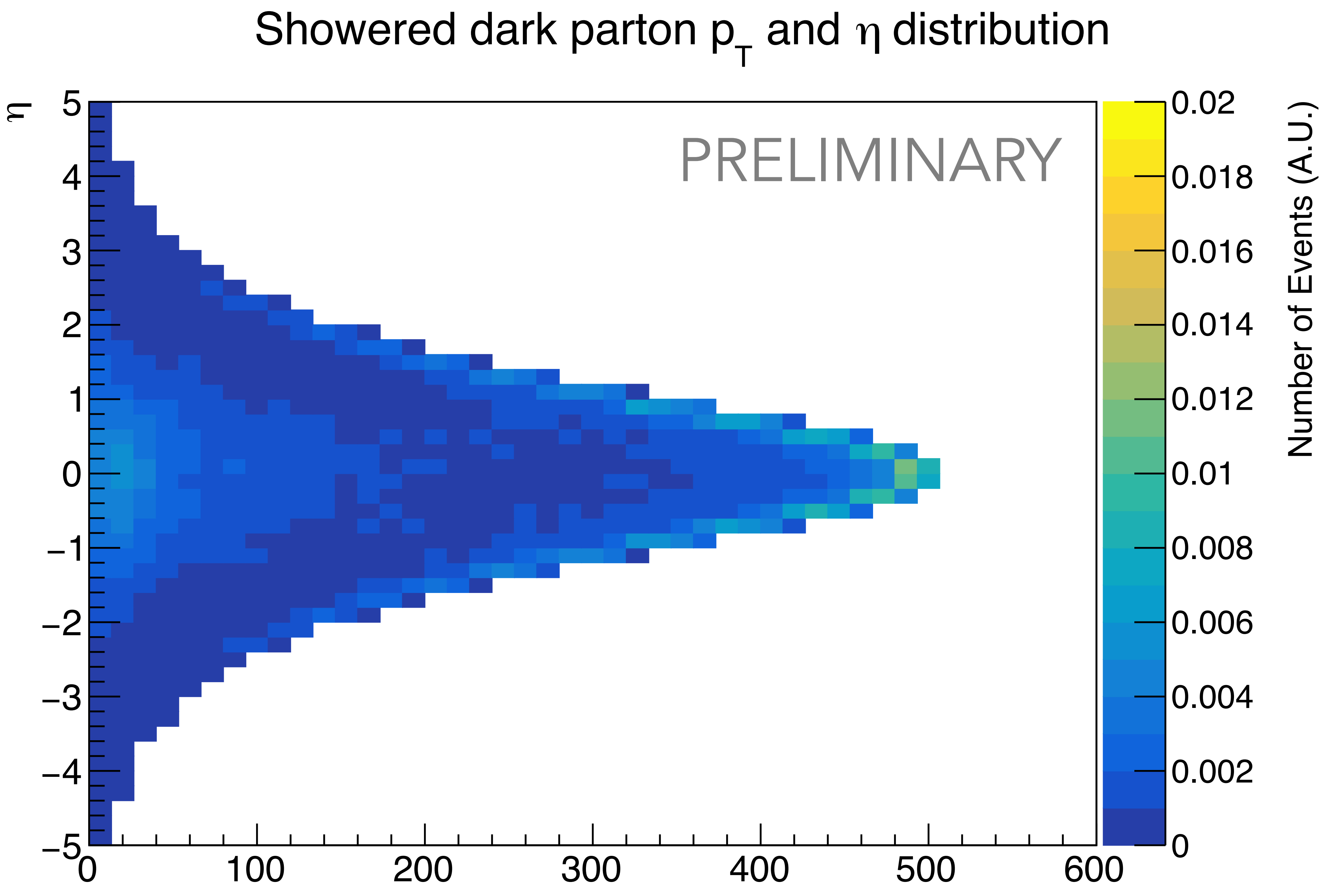

$\Lambda = 5$ GeV , $N_F = 16$

Simulated with a custom Pythia 8.307 with benchmark:
$e^+e^- \to Z' \to q_D\overline{q_D}$,
$\sqrt{s} = 1.1 M_{Z'} = 1.1$ TeV,
hadronisation off ,
$\Lambda = 5$ GeV , $N_C = 3$.
Cutoff at $Q = 1.1\Lambda$.

- At around N_F/N_C ~5, there is a transition in the $p_T — \eta$ plane from the majority of dark partons being soft to a majority being hard - the majority of dark partons are initial dark quarks.
- For every dark parton splitting, the two resulting dark partons share the transverse momentum p_T meaning the more splittings, the softer the final state dark partons. In the IRFP region, the average $\eta \to 0$ as $N_F/N_C \to 5.5$, more events are back-to-back with respect to the beam line.

pT-eta distributions

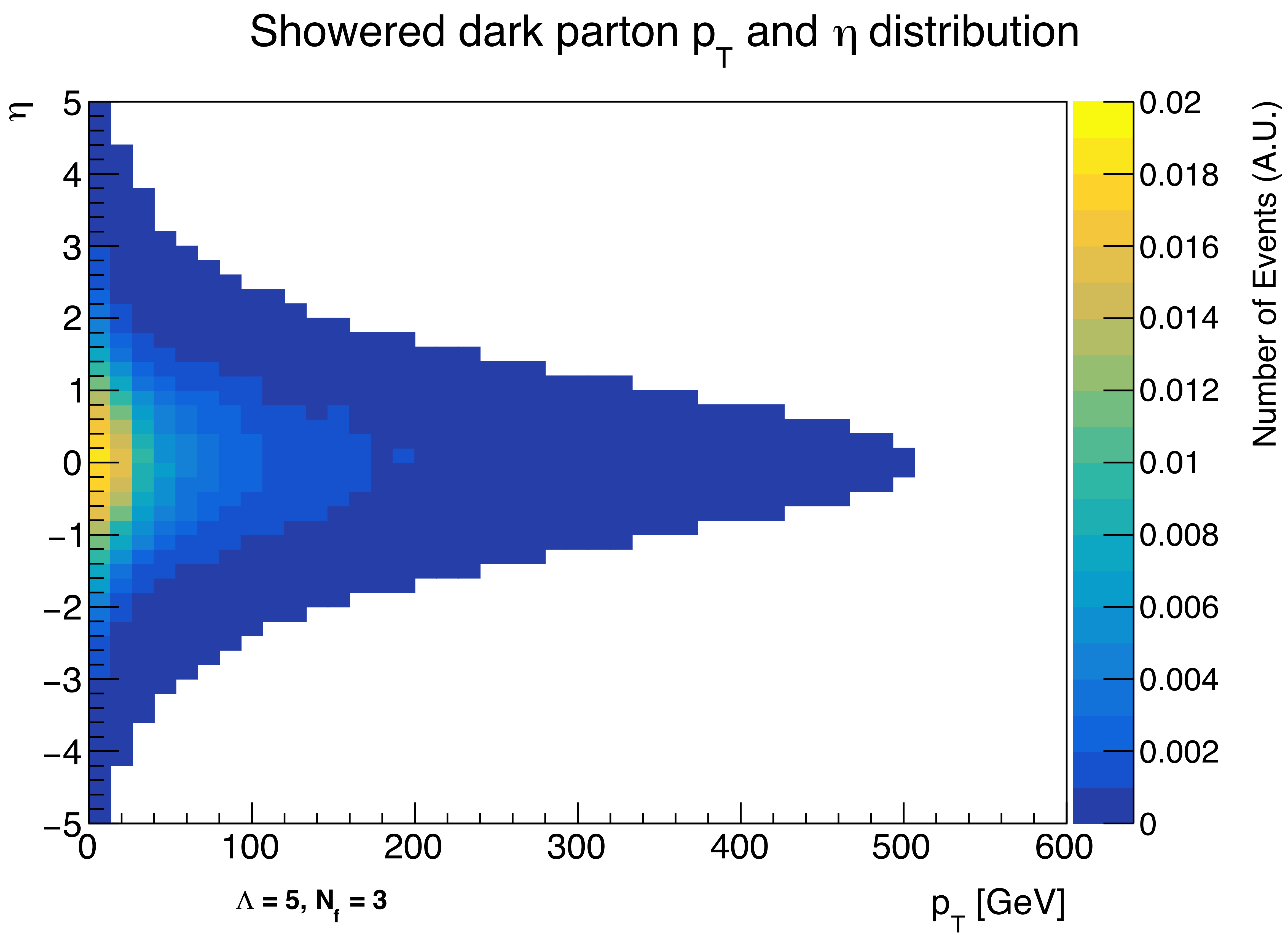

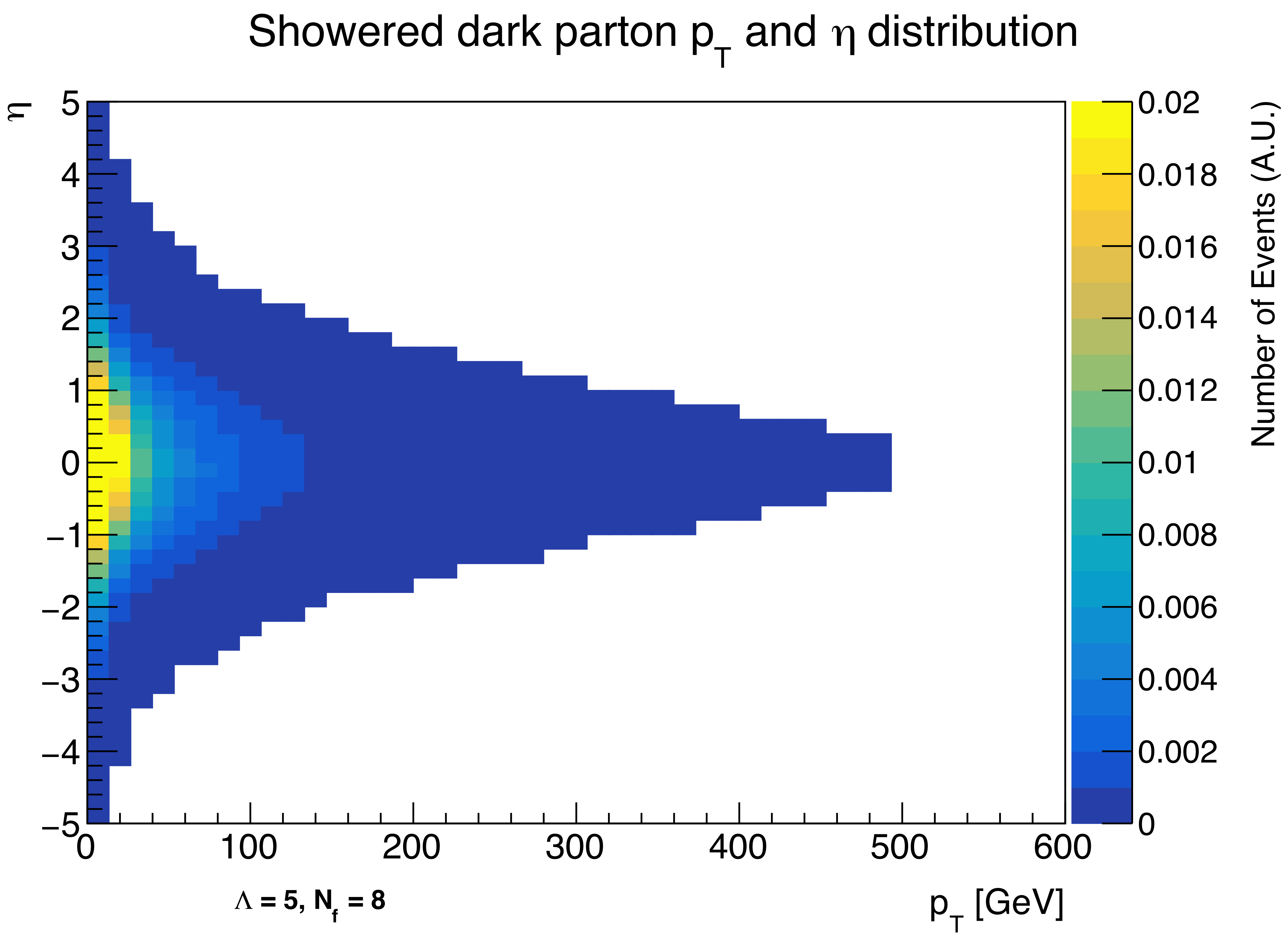

pT-eta distributions

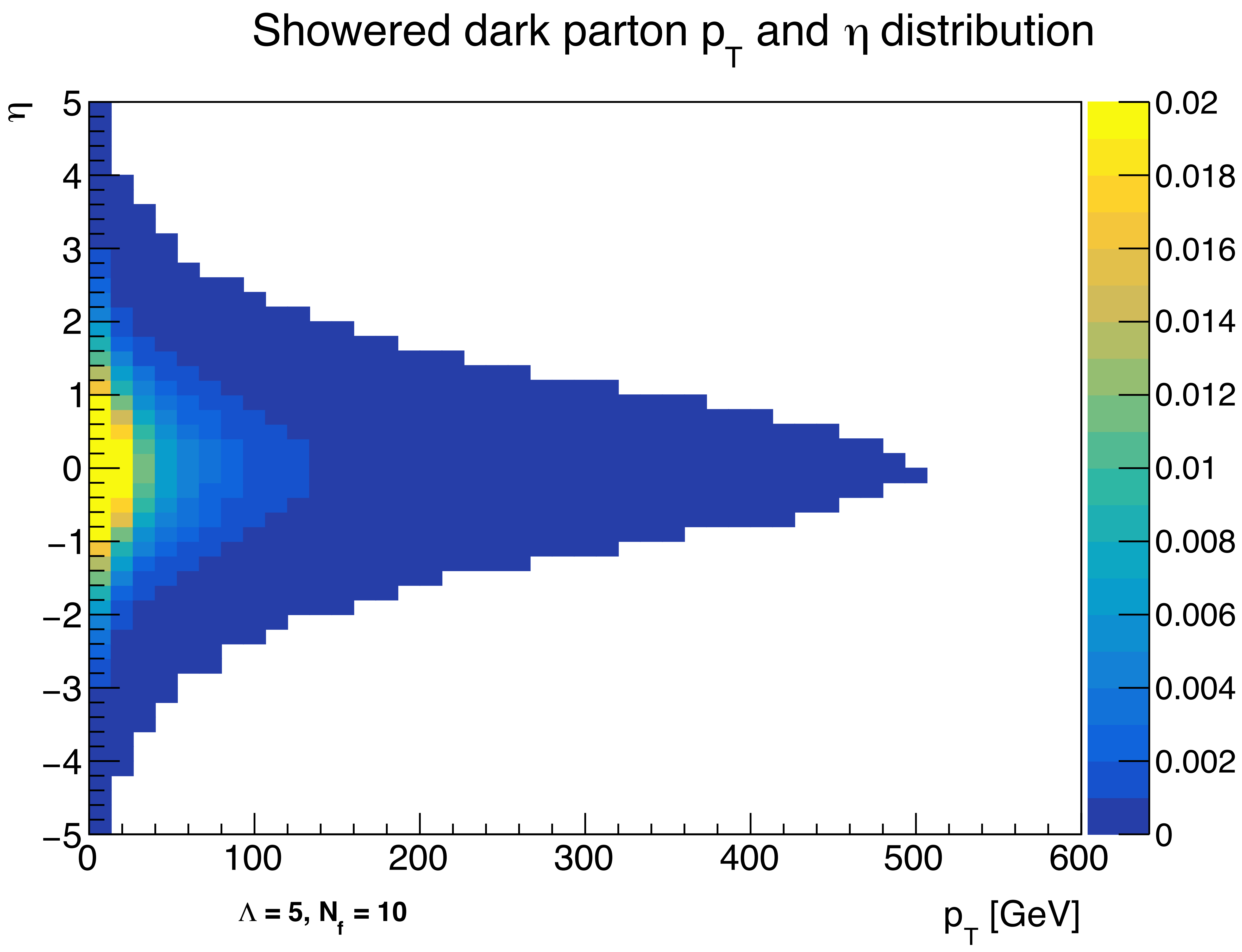

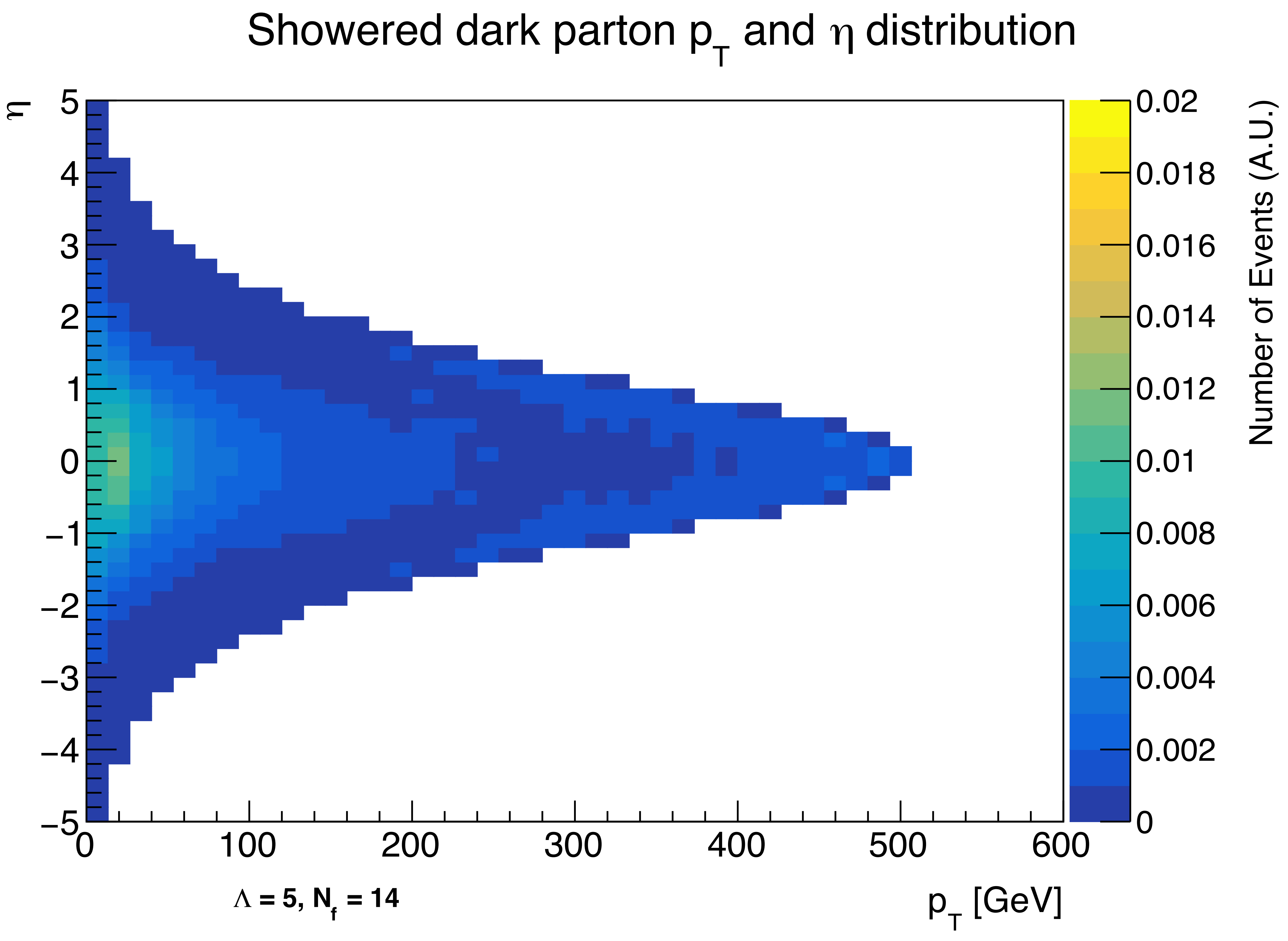

pT-eta distributions

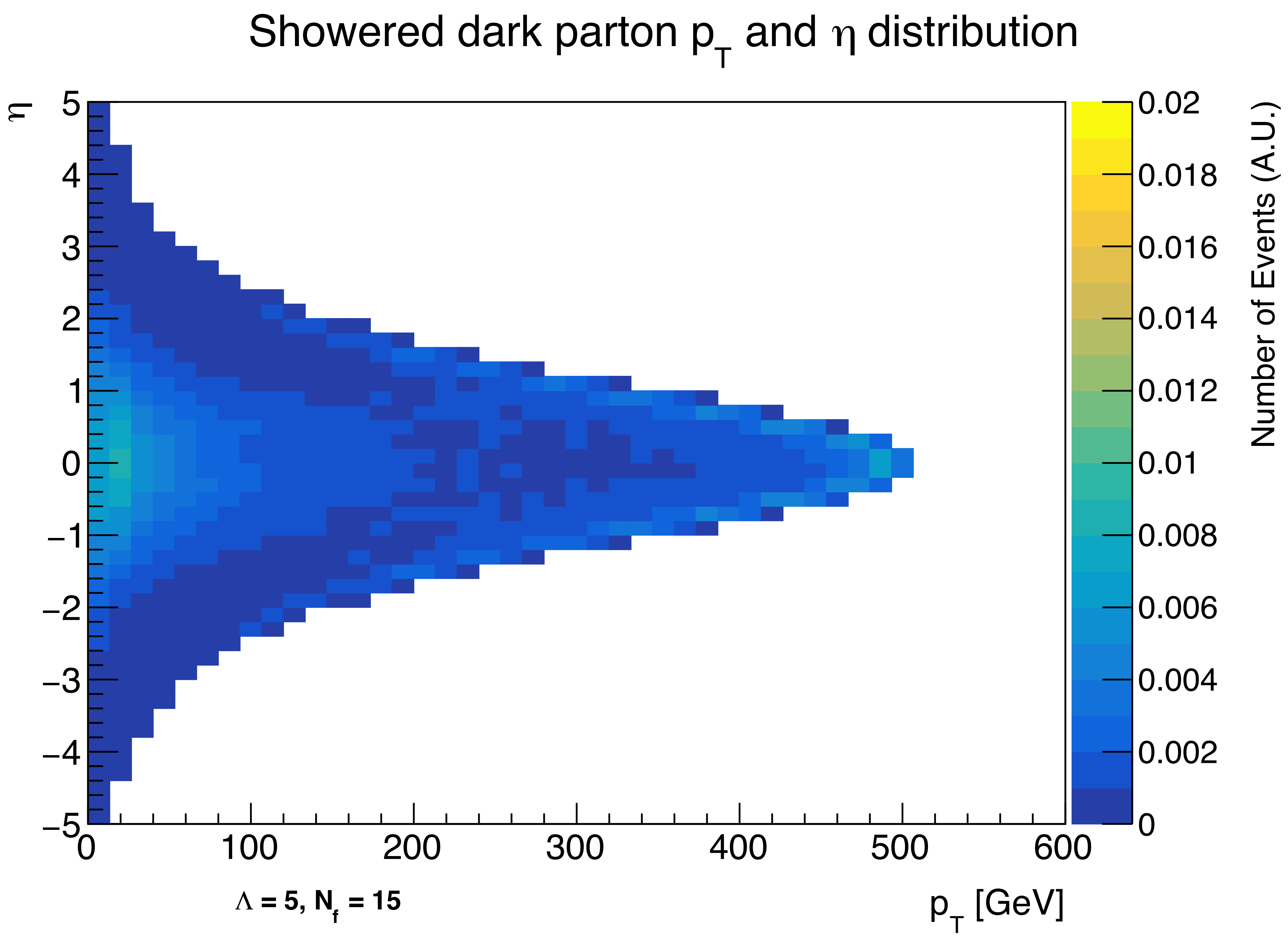

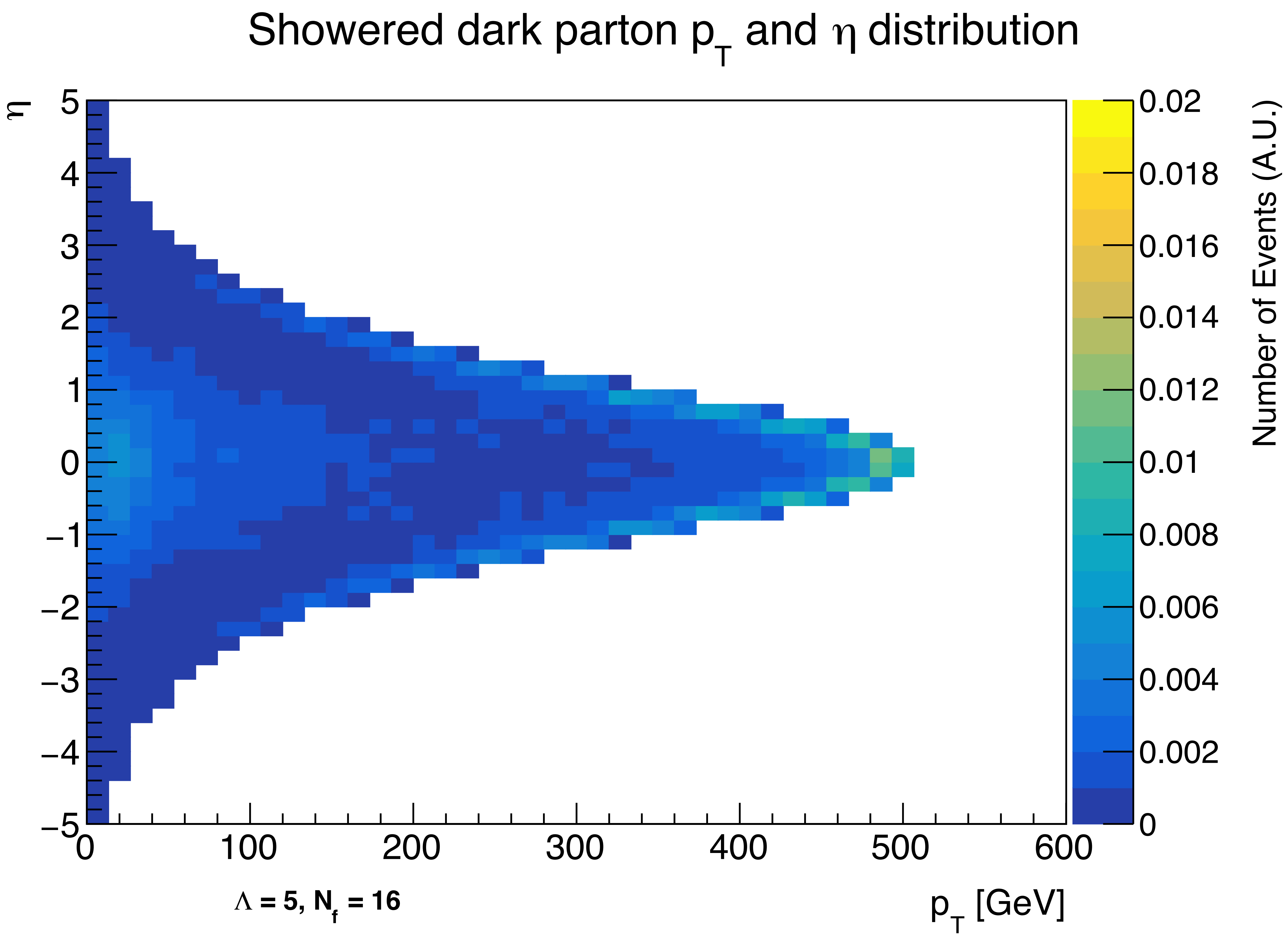

Future issues: Three-loop

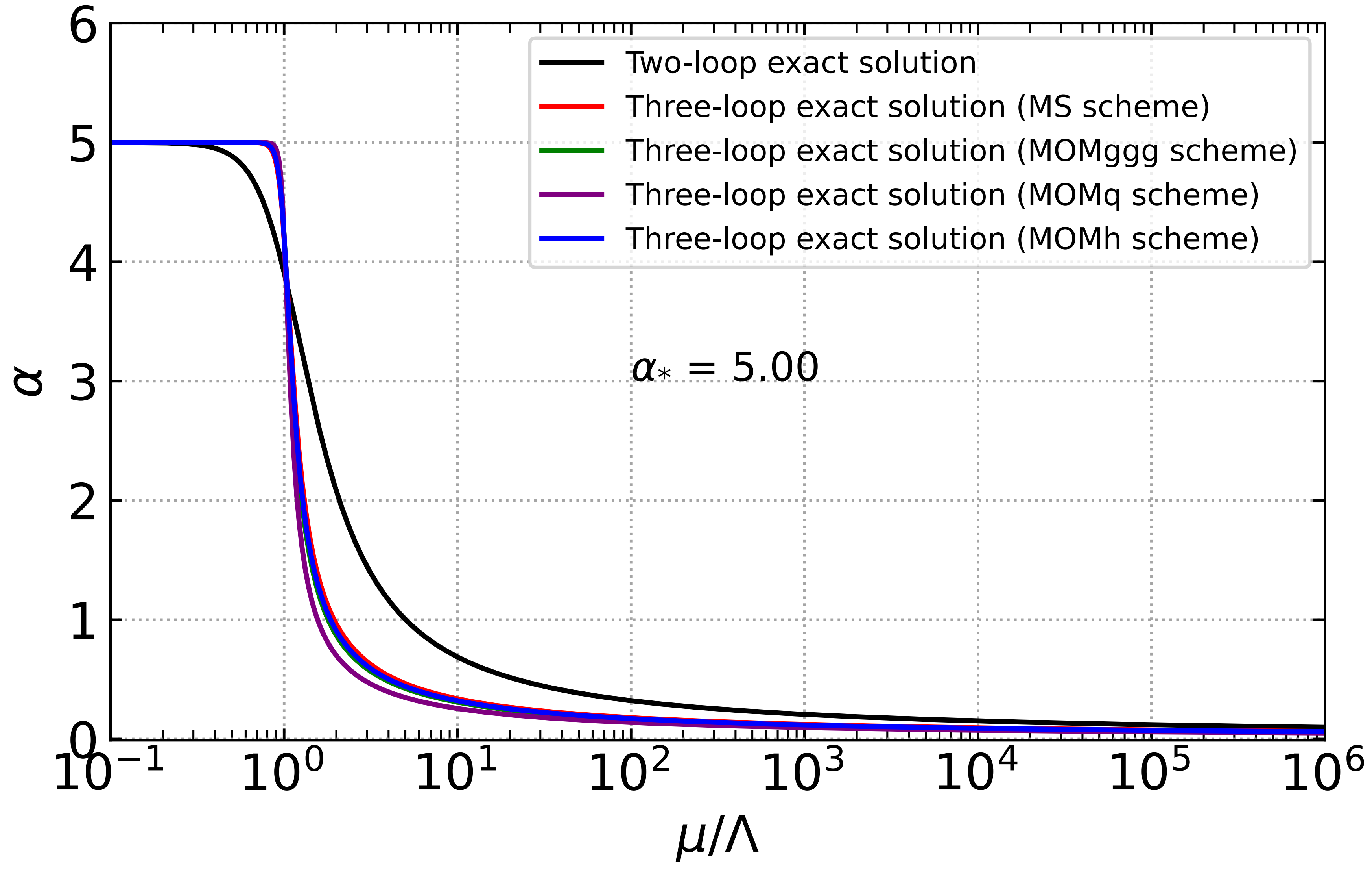

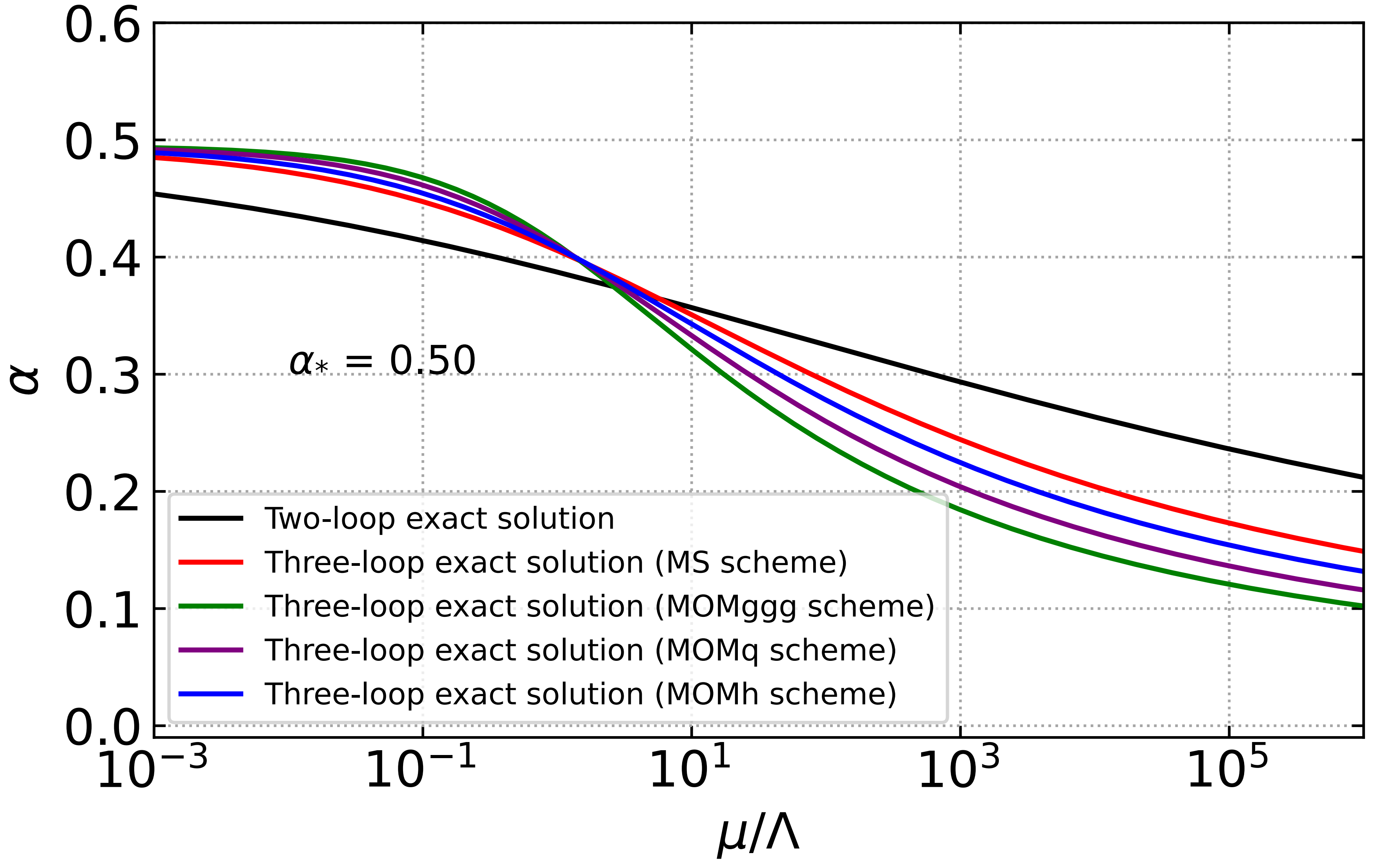

- Going to three-loop order adds additional complications not present at two-loop order. Although one is able to derive large μ/Λ and other approximations, as well as interpolate between them, there are still some areas where differences arise.
- Among the $\overline{MS}$ and MOM schemes, differences in the β coefficients only arise at three-loop order. In general, when varying N_F/N_C IRFPs appear much earlier than at two-loop.
- Holding α_* fixed may be more appropriate when comparing two- and three-loop. Preliminary results suggest that major deviations between loop orders (occurring near $\mu/\Lambda = \mathcal{O}(10)$) for large IRFPs, but no deviations between schemes.
- For small IRFPs, there are significant deviations in both loops and scheme changes for a wide range of μ/Λ. For very small IRFPs ($\ll 1$) there are no observed differences between schemes or between loop orders.

Three-loop

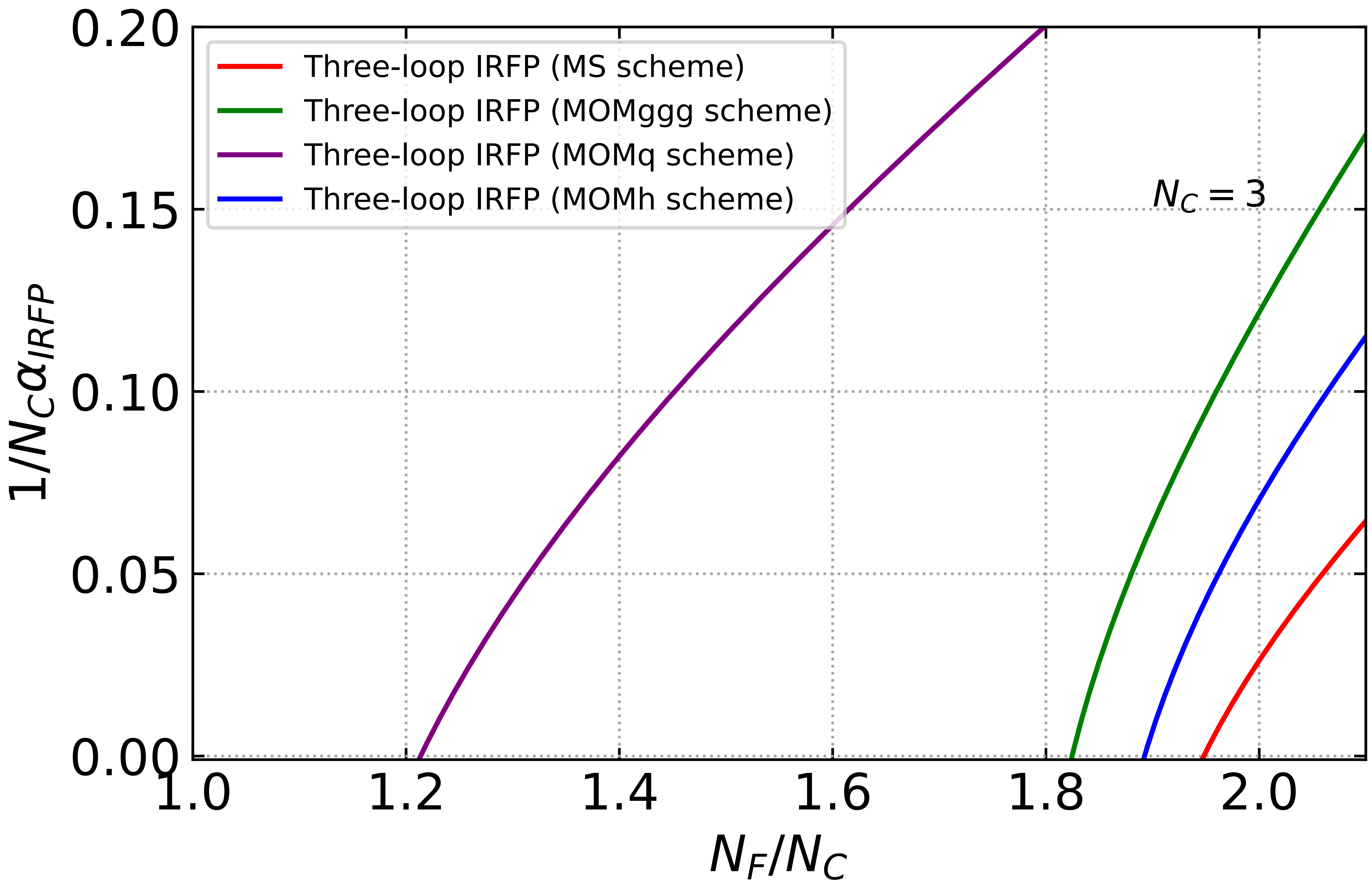

Three-loop IRFP (MS scheme)
Three-loop IRFP (MOMggg scheme)
Three-loop IRFP (MOMq scheme)
Three-loop IRFP (MOMh scheme)
$N_C = 3$
$1/N_C\alpha_{IRFP}$
N_F/N_C
0.00
0.05
0.10
0.15
0.20
1.0
1.2
1.4
1.6
1.8
2.0

PDG approximation at small IRFPs

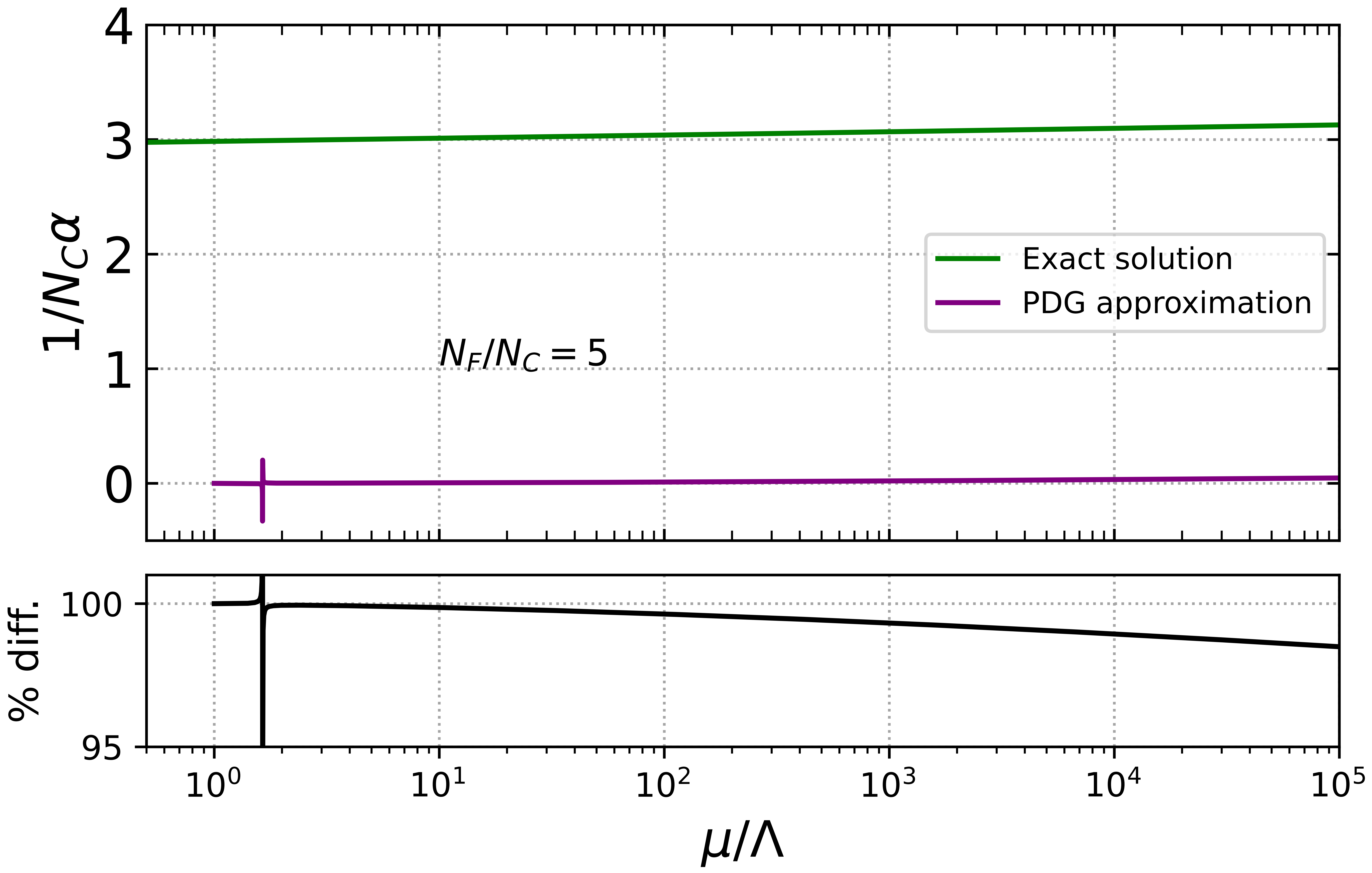

One-loop vs two-loop

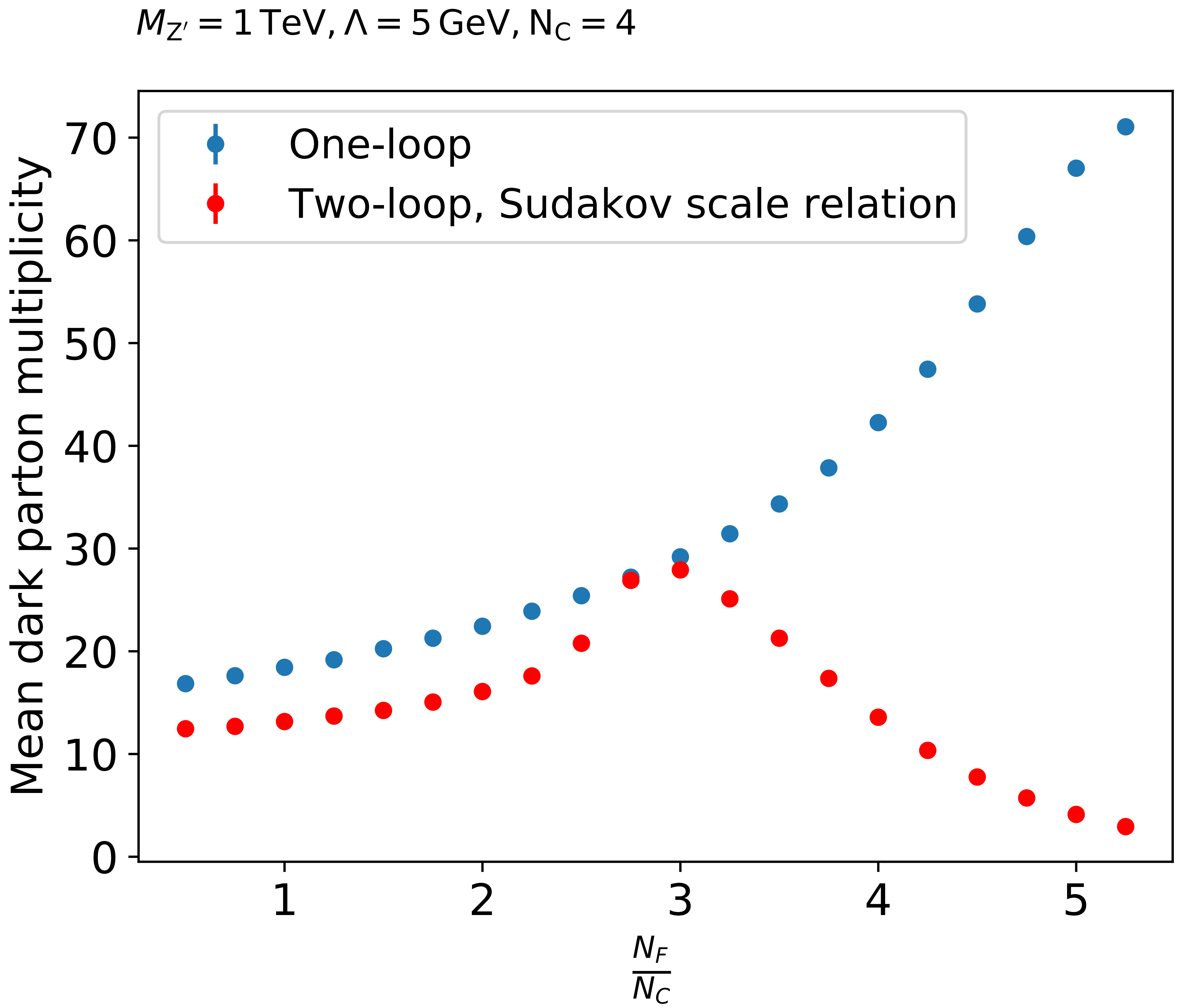

Veto factor - two-loop running

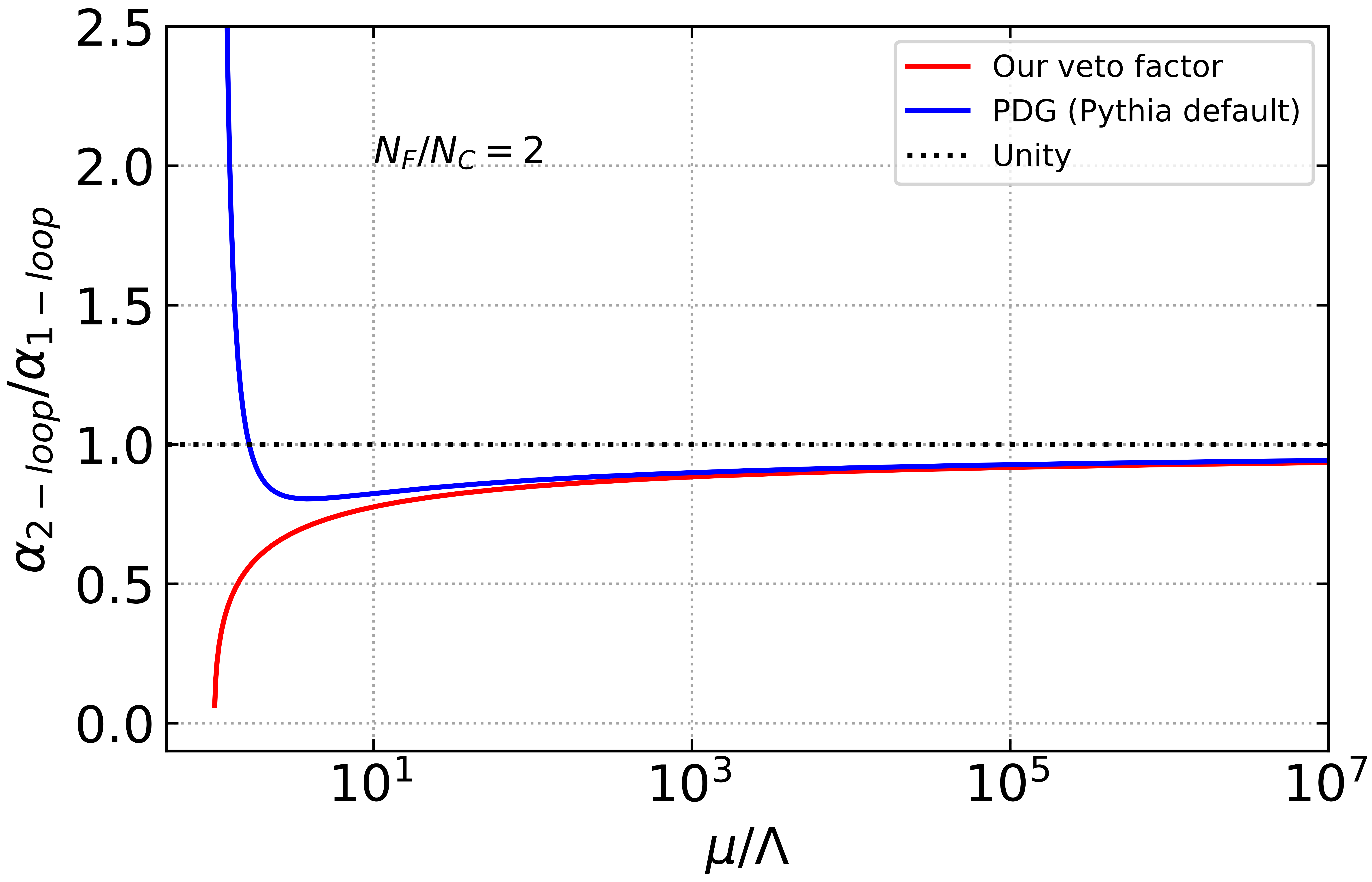

Veto factor - two-loop running

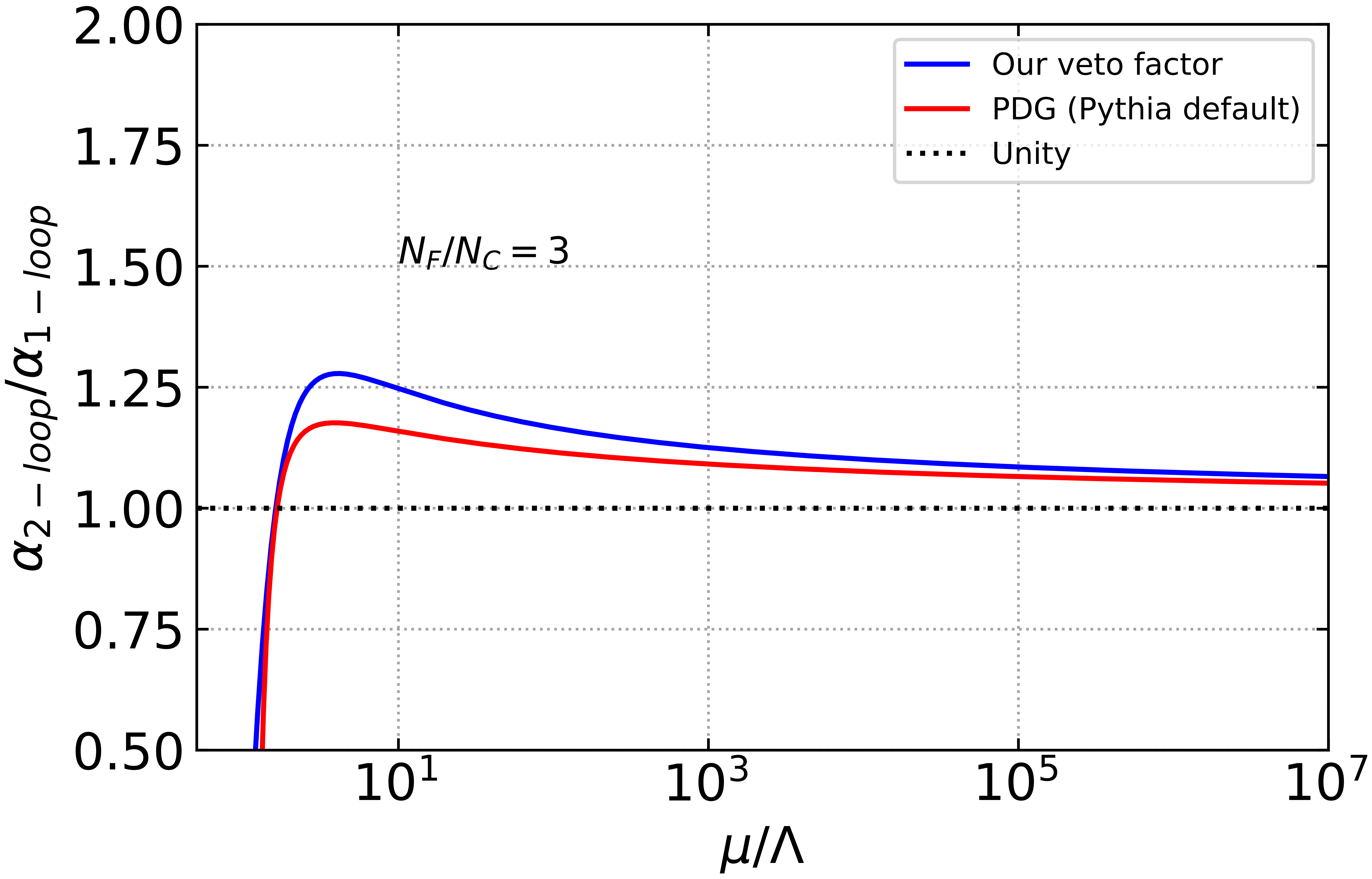

Veto factor - two-loop running

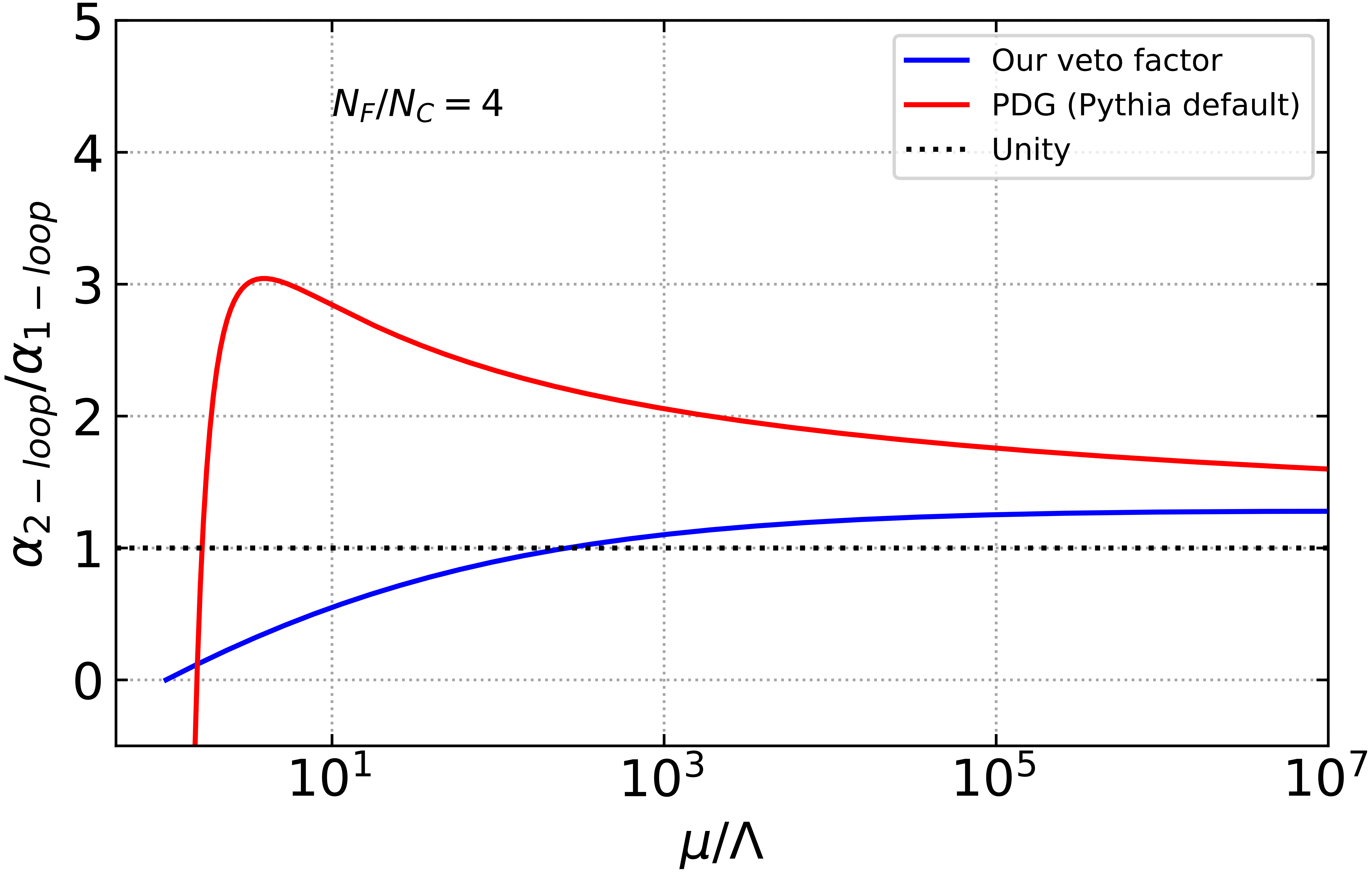

PDG approximation at small IRFPs

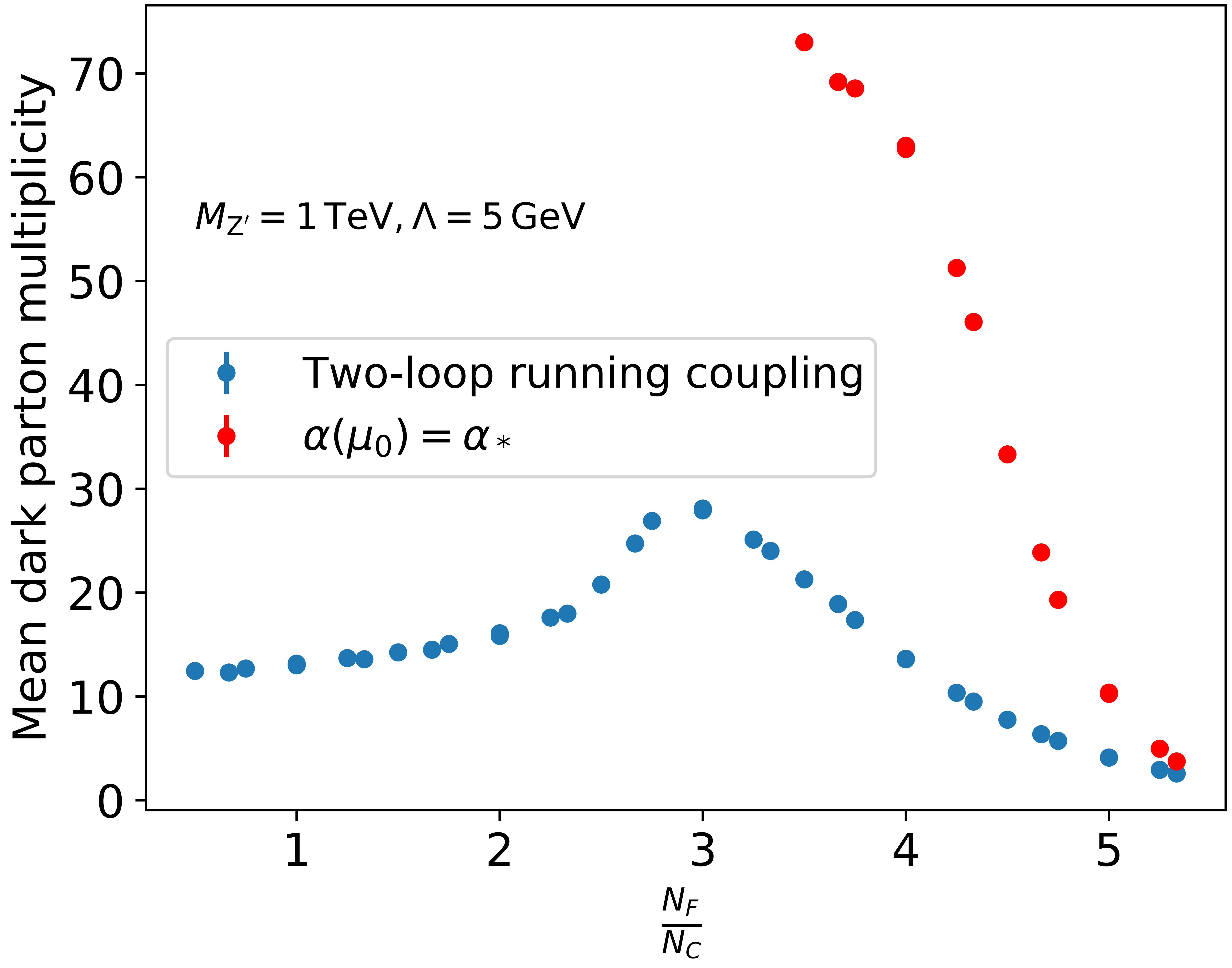

Dark parton multiplicity in pp collisions

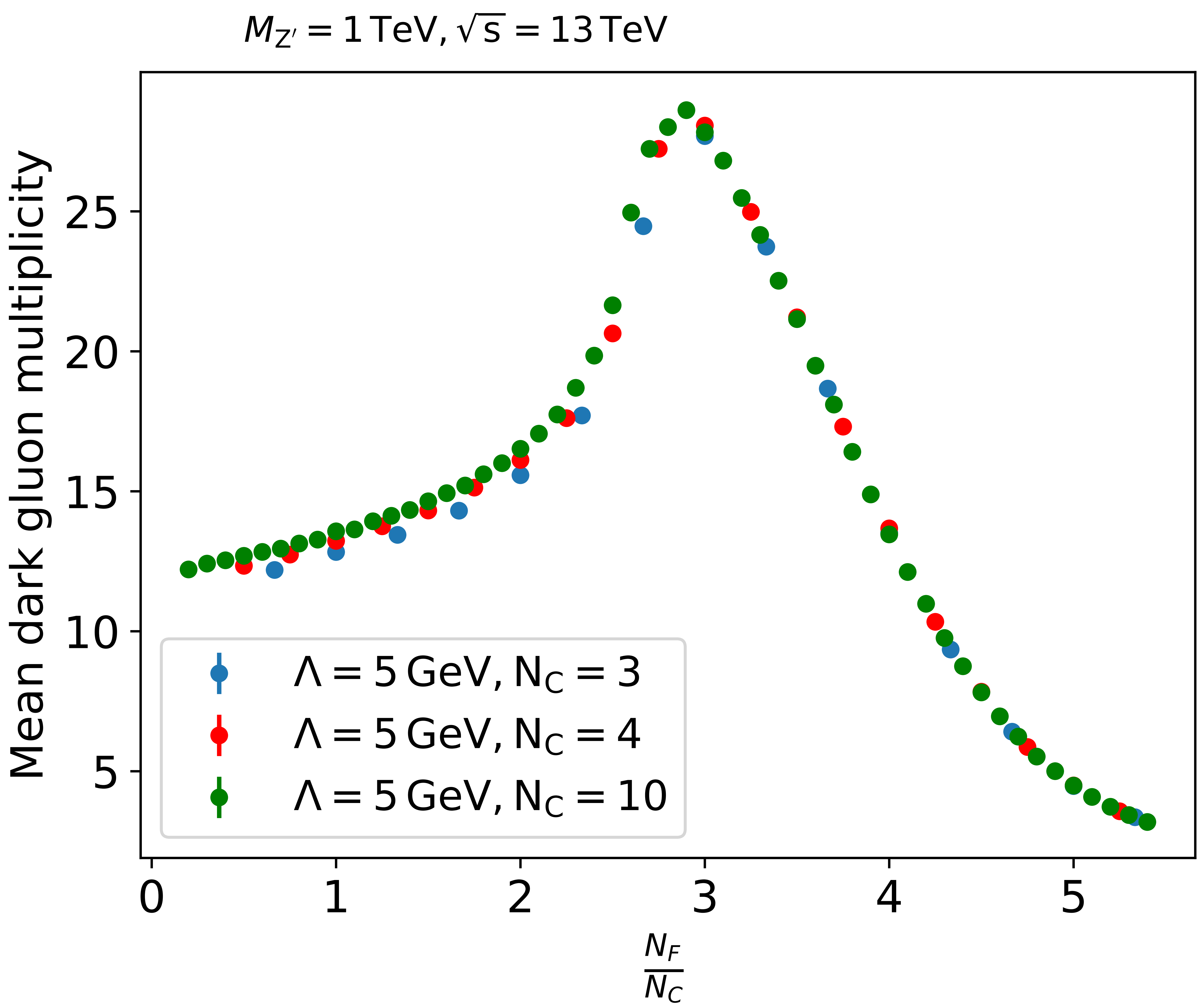

Average dark parton multiplicity

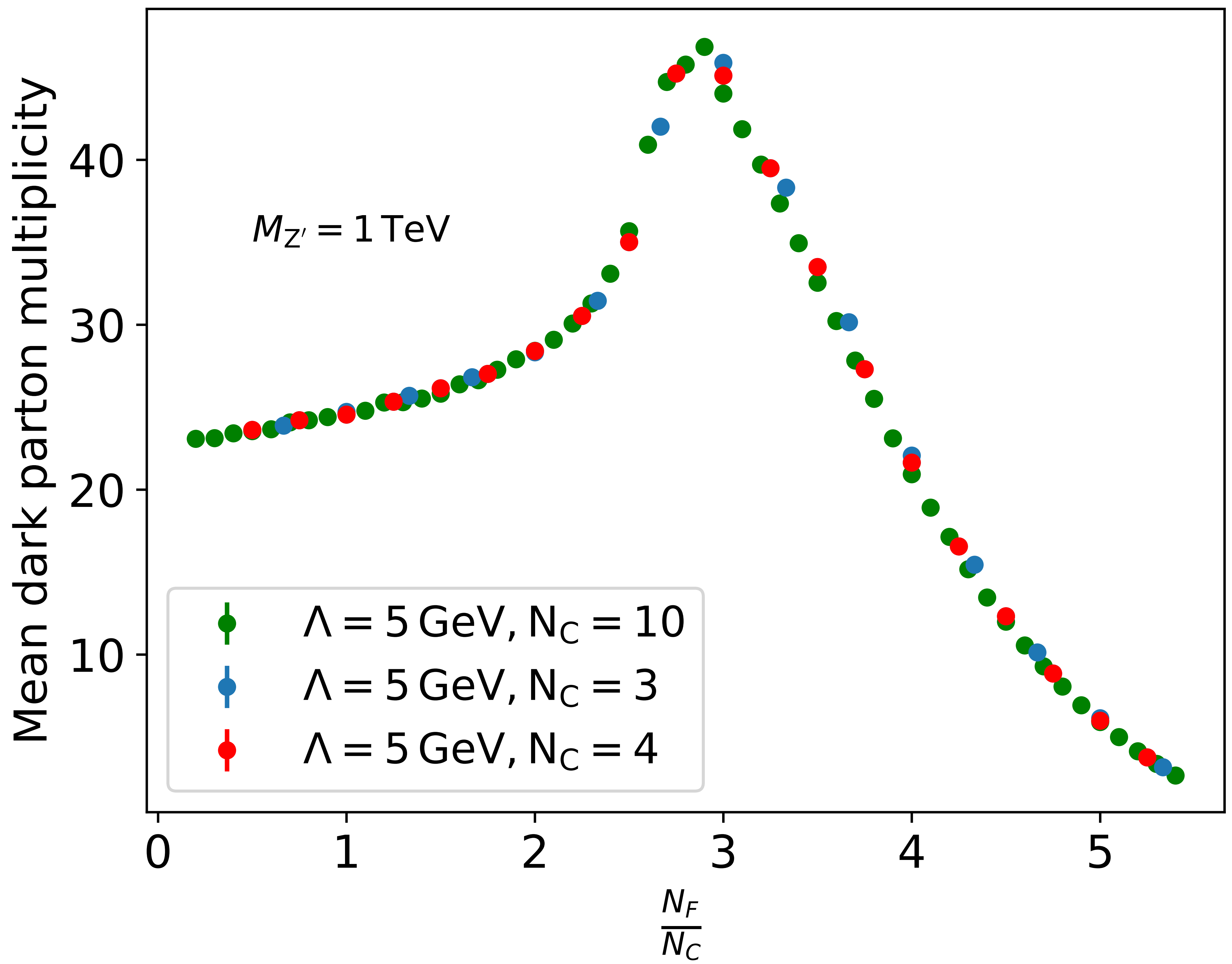

Simulated with a custom Pythia 8.307 with benchmark: $e^+e^- \to Z' \to g_D g_D$, $\sqrt{s} = 1.1 M_{Z'} = 1.1$ TeV, hadronisation off , $\Lambda = 5$ GeV , $N_C = 3$. Cutoff at $Q = 1.1\Lambda$.

- Since parton splitting probability is proportional to α, it thus vanishes as $N_F/N_C \to 5.5$. Hence there is very little splitting at N_F/N_C ~ 5 and average parton multiplicity tends to 2 - the 2 initial dark quarks.

$$d\mathscr{P}_a\left(\xi, Q^2\right) = \frac{dQ^2}{Q^2}\frac{\alpha(Q^2)}{2\pi}\sum_{b,c} P_{a\to bc}(\xi)d\xi$$

- Maximum of the dark parton multiplicity distribution occurs at $N_F/N_C = 2.9$ and not $N_F/N_C = (N_F/N_C)_*$.

Comparison with PDG and IRFP veto algorithm

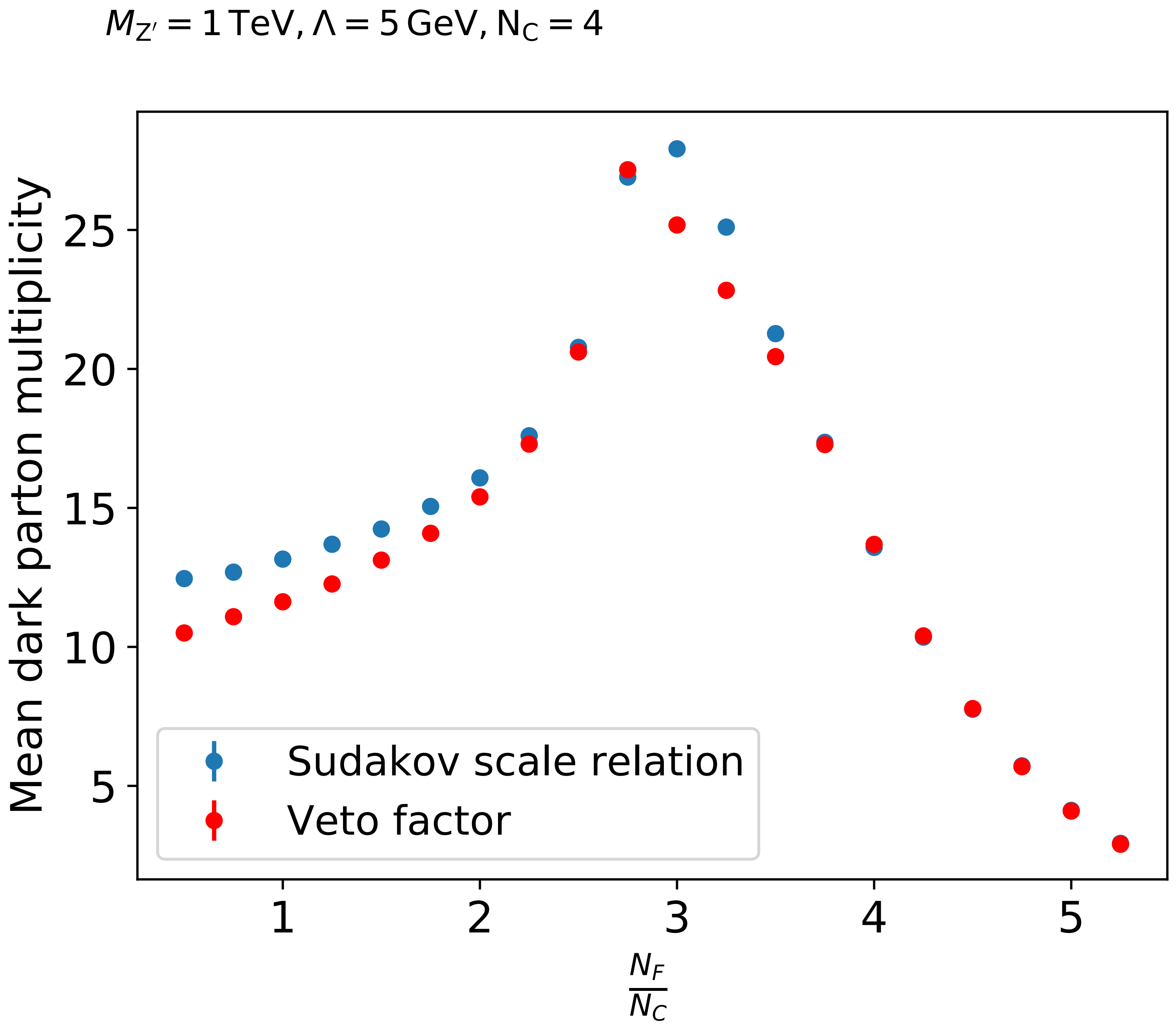

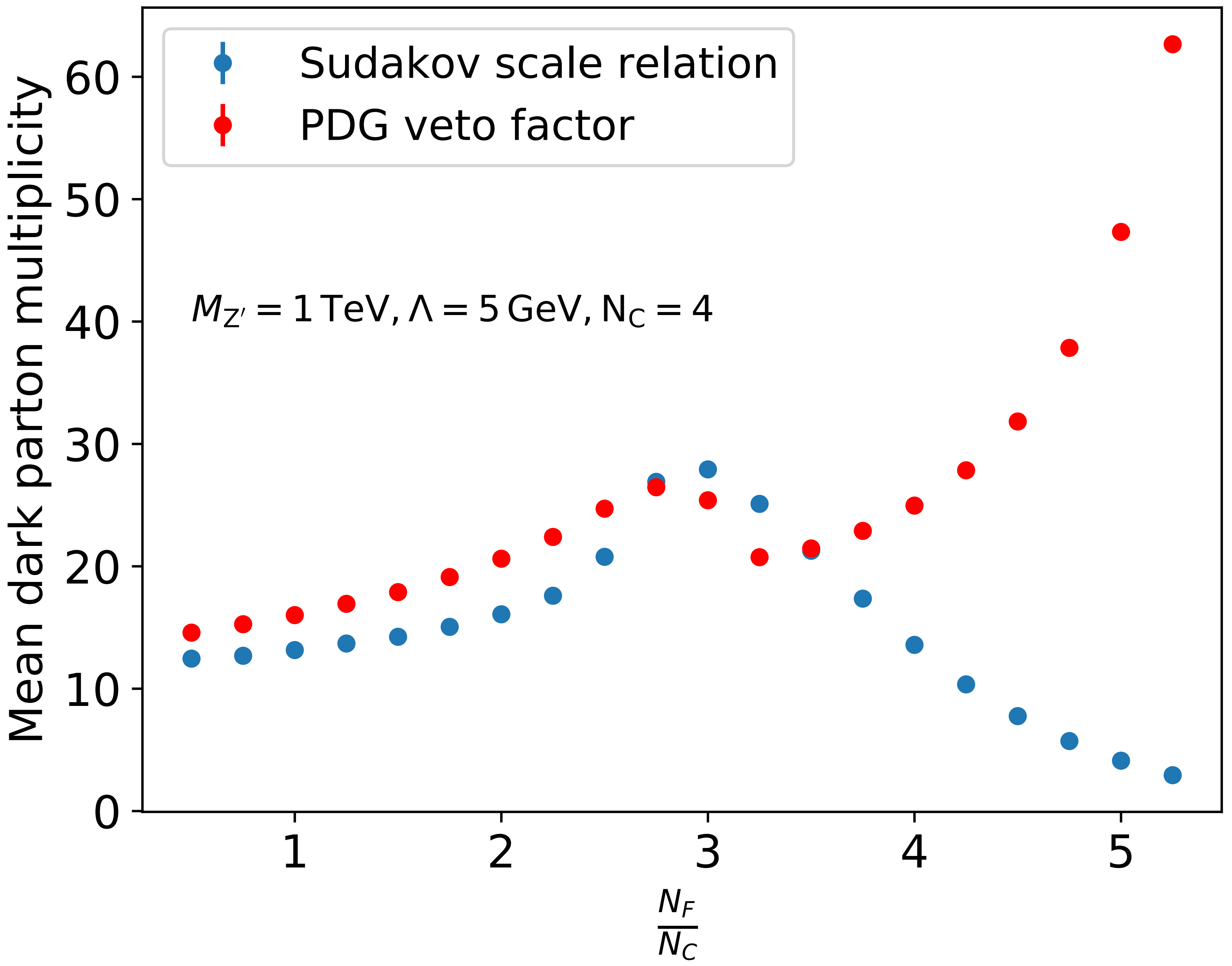

Simulated with a custom Pythia 8.307 with benchmark: $e^+e^- \to Z' \to q_D\overline{q_D}$, $\sqrt{s} = 1.1M_{Z'} = 1.1$ TeV, hadronisation off , $\Lambda = 5$ GeV , $N_C = 3$. Cutoff at $Q = 1.1\Lambda$.

- The IRFP veto algorithm underestimates estimates the parton multiplicity in the QL region. In the CW region, for large IRFPs, it misses the correct maximum whilst for small IRFPs, the veto algorithm works and results match the Sudakov implementation.
- The original two-loop veto algorithm that used the PDG running coupling overestimates the parton multiplicity in the QL region. In the CW region, the PDG multiplicity curve replicates the IRFP veto algorithm for large IRFPs, but completely fails for small IRFPs since the effects of the IRFPs become significant in this region.